BL1A, BL8B1

Electronic Structure Change of $LiNi_{1/2}Mn_{1/2}O_2$ Cathode Materials for Lithium-Ion Secondary Batteries from Metal L-Edge and Oxygen K-Edge Spectroscopy

Y. Arachi[1], H. Kobayashi[2], H. Maeda[1], T. Asai[1]
[1]*Faculty of Engineering, Kansai University, Osaka 564-8680, Japan*
[2]*Research Institute for Ubiquitous Energy Devices, AIST, Ikeda, Osaka, 563-8577 Japan*

In order to establish the materials design for the Lithium ion batteries, we have employed the variety of measurement techniques and specifically, examined the crystal structure and electronic structure using X-ray, neutron diffraction and XAFS measurements. The absorption peaks of transition metal $L_{2,3}$ edges can directly obtain the information of unoccupied 3*d* states. Because the quadrupole transitions from 1*s* to 3*d* (K edge) are much weaker than dipole from 2*p* to 3*d*. In addition, O K edge spectra provide bonding interactions between metal and oxygen due to the overlapping between 3*d* of metal and 2*p* orbital of oxygen. In our field, the alternatives to conventional $LiCoO_2$ cathode material have been extensively searched due to small natural deposits of Co and its toxicity. $LiNi_{0.5}Mn_{0.5}O_2$ with layered-NaCl type structure proposed as one of a promising material manifests fascinated character such as a good cycleability and reversible capacity of 150 mAh/g within the voltage range of 3.0 to 4.3 V, which corresponds to one-half of theoretical capacity (280mAh/g). Recently, we have synthesized the material by using ion exchange reaction, which showed the suppression of Li/Ni disordering in the layered structure. In this study, the electronic structural changes were observed by XANES spectra of Ni, Mn L-edges and O K-edge respectively and the charging behavior was examined.

$LiNi_{1/2}Mn_{1/2}O_2$ was prepared by ion exchange reaction of $NaNi_{1/2}Mn_{1/2}O_2$ as a precoursor. $NaNO_3$ and precipitates of Ni, Mn hydroxides were mixed and then calcinated at 600°C for 12h. The obtained powders were pressed and sintered at 900°C for 12h in air. The ion exchange reaction was carried out in Li molten salt(LiCl: $LiNO_3$=1:1 (mol), eutectic point = 244°C) at 280-450°C for 0.1 to 10 h. and de-lithiated samples were electrochemically and chemically prepared. The former was used by coin-type cells with Li/1M $LiPF_6$ in EC:DEC(1:1)/samples and the latter was by the chemical oxidants, ammonium persulfate as the following reaction:

$$S_2O_8^{2-} + 2e^- \rightarrow 2\ SO_4^{2-}$$

$$LiNi_{1/2}Mn_{1/2}O_2 \rightarrow Li_{1-x}\ Ni_{1/2}Mn_{1/2}O_2 + xLi^+ + xe^-.$$

X-ray absorption measurements at the Ni, Mn L-edges and O K-edge by total electron yield were performed on BL1A, BL8B1 and occasionally BL4B.

$LiNi_{1/2}Mn_{1/2}O_2$ showed a single phase adopted the a-$NaFeO_2$ structure like as $LiCoO_2$. Neutron diffraction measurements demonstrated that the lattice parameters are a = 2.8922(0) Å and c = 14.31(5) Å and Ni occupancy at Li site, g_{Ni} is 0.028. The chemical composition can be expressed as $[Li_{0.97}Ni_{0.03}]_{3a}[Li_{0.03}Ni_{0.47}Ni_{0.50}]_{3b}O_2$, referring to the Wyckoff positions 3*a* and 3*b* with space group *R*3m. The structure depended on the ion-exchange reaction temperature and time. As increased the reaction temperature and time, the Li/Ni disorder became remarkable. The irreversible capacity was improved by the ion-exchange. Figure 1 shows the selected XANES spectra of O K-edge for chemically oxidized $Li_{1-x}Ni_{0.5}Mn_{0.5}O_2$. The notation from deLi1 to deLi4 corresponds to the reaction time of 0.1 to 1.0 h at various steps. These peaks indicate transition metals 4*sp*. A peak of **A** slightly shifted towards lower energy, while maintaining the peak position of **B**. As the sample oxidized, the orbital of O 2*p* introduced a hole. On the other hands, the results of Ni L-edge showed a slightly higher shift and that of Mn L-edges showed no chemical shifts for all the samples. On the basis of these results, we are constructing the band structure and investigating the charging mechanism for this material.

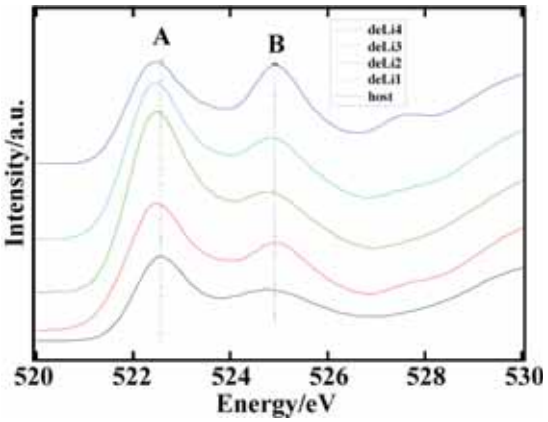

Fig. 1. O K-edge XANES spectra of chemically oxidized $Li_{1-x}Ni_{1/2}Mn_{1/2}O_2$.

BL1A

Mo L_{III}-Edge XANES Study of Catalytically Active Mo Sites on H-MFI for Methane Dehydriaromatization with Hydrogen

H. Aritani[1], H. Shibasaki[1], N. Naijo[1], K. Takanashi[1], K. Nagashima[1], A. Nakahira[2]
[1]*Faculty of Engineering, Saitama Institute of Technology, Fukaya 369-0293, Japan*
[2]*Graduate School of Engineering, Osaka Prefecture University, Sakai 599-8531, Japan*

Introduction

Mo-modified H-MFI catalysts show high activity for dehydroaromatization of methane in absence of oxygen. In this reaction, reduction of Mo species is brought about in contact with methane in initial step, and reduced Mo ions react methane to form carbide and/or oxycarbide species in next step. It has been accepted that the carbide and/or oxycarbide species are the active center for dehydroaromatization of methane. However, deactivation cannot be avoided by carbon deposition. Hydrogen co-feed with methane is effective for suppression of coking. On the other hand, excess hydrogen may affect a reduction of Mo species during the reaction, and decrease of active Mo-oxycarbide species may give low reactivity. Thus the effect of hydrogen with methane is very important to give an effect on Mo states. This study addresses the effects of hydrogen co-feed on methane dehydroaromatization over Mo/H-MFI catalysts. Mo L_{III}-edge XANES studies were introduced to characterize the active Mo species on H-MFI before/after the methane dehydroaromatization in the absence/presence of hydrogen.

Experimental

Catalysts were prepared by impregnation of H-MFI support with $MoO_2(acac)_2$–$CHCl_3$ solution, and followed by drying overnight and calcination at 773 K. H-MFI supports were synthesized hydrothermally at 413 K for a week, and followed by ion-exchange and calcination at 873 K. Mo L_{III}-edge XANES spectra were measured in BL1A of UVSOR-IMS in a total-electron yield mode. Photon energy was calibrated by using Mo metal-foil at Mo L_{III}-edge, and normalized XANES spectra and their second derivatives were obtained. Catalytic activity was evaluated in a fixed bed flow reactor. Each catalyst (0.25 g) was placed in a quartz-tube reactor, and pretreated in He–H_2(0-1%) flow (30 mL min^{-1}) at 973 K for 1 h. Then CH_4(20%)–H_2(0-3%)–He reactant gas was fed at 973 K (30 mL min^{-1}: SV = 7.2 L g^{-1} h^{-1}). Products were analyzed by online GC. Amount of coking carbon was evaluated by thermogravimetry.

Results and Discussion

For the dehydroaromatization in our study, 5.0

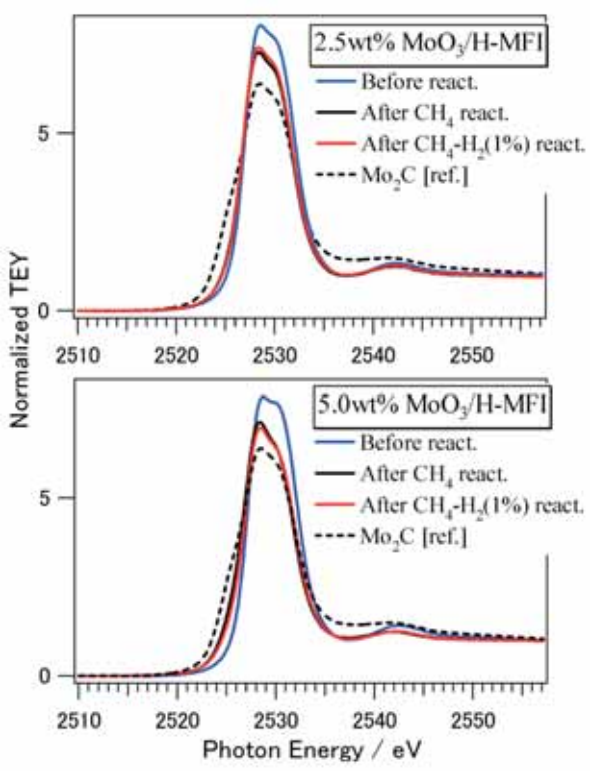

Fig. 1. Mo L_{III}-edge XANES of Mo/H-MFI before/after methane dehydroaromatization.

Mo-loading on H-MFI (Si/Al_2=72) showed a maximum C_6H_6 yield under no additives with CH_4(20%) reactant. H_2(1%) co-feed with CH_4 gave low deactivation, indicating the suppression of coking. But excess H_2 (in 1.5 %) enhanced the deactivation. H_2 pretreatment brought about low activity in the initial step. These results suggest that both inhibition of excessive Mo reduction and suppression of coking on H-MFI relate to the highly catalytic activity for methane dehydroaromatization. The results of L_{III}-XANES (Fig. 1) and their 2nd derivatives suggests the coexistence of Mo^{2+} and oxidized ions after the reaction with CH_4 or CH_4-H_2(1%). On the other hand, Mo^{2+} is dominant after H_2(1%)-He pretreatment. These results indicate that H_2 co-feed with CH_4 does not affect the reduction of active Mo sites, and H_2 pretreatment (without CH_4) brings about the reduction to form Mo^{2+} species in major. And thus, it is concluded that active Mo species consist of Mo^{2+}-oxycarbide species on H-MFI support.

BL1A

Local Structure Analysis of Composite Oxide Electrodes of Dye-Sensitized Solar Cells by XAFS Method

S. Iwamoto[1], Y. Sazanami[1], T. Kadata[1], H. Ozaki[1], W. Hong[1], H. Kanai[1], M. Inoue[1], T. Inoue[2], T. Hoshi[2], K. Shigaki[2], M. Kaneko[2]

[1]*Graduate School of Engineering, Kyoto University, Katsura, Kyoto 615-8510, Japan*

[2]*Nippon Kayaku Co.Ltd., 31-12, Shimo 3-chome, Kita-ku, Tokyo 115-8588, Japan*

Dye-sensitized solar cells (DSSCs) attract great attention because of their high photovoltaic conversion efficiency, simple fabrication process, and low material and production costs [1]. In the last two decades, noticeable improvement in short-current density (J_{sc}) and fill factor (*ff*) has been attained; however, only a slight increase has been accomplished with regard to open-circuit voltage (V_{oc}). In usual DSSCs, titanium oxide and iodide-based solution are used as the electrode and electrolyte, respectively. As the maximum V_{oc} is determined by the difference between the Fermi level of the electrode under illumination and the redox potential of the electrolyte, using these two components, Voc is definitely limited to ca. 0.9 V. Recently, we found that a DSSC consisting of a conjugated acid organic sensitizer and a nanocrystalline Mg-containing TiO_2 generated quite a high V_{oc} of 1 V [2]. In this study, Mg K-edge XANES of various Mg-containing samples were measured to elucidate the local structure of the Mg-modified titanias.

Mg-modified titanias (Mg(x)-TiO_2, where x is Mg/Ti charged ratio) were prepared by the thermal reaction of mixtures of titanium tetraisopropoxide and magnesium acetate tetrahydrate in 1,4-butanediol at 300 ºC (Glycothermal method) [3]. X-ray diffraction (XRD) analysis shows that the obtained products of $x \leq 0.2$ were nanocrystals with the anatase structure. The unit cell parameters of these Mg-modified titanias were increased with increasing the amount of the Mg addition, indicating that Mg^{2+} ions were incorporated in the anatase structure. In Fig. 1, Mg K-edge XANES of various samples are shown. The spectra of Mg-modified TiO_2 samples prepared by an impregnation method (designated as Mg(x)-TiO_2(imp)) suggested the presence of MgO phase. On the contrary, the spectra of Mg(x)-TiO_2 samples preapered by the glycothermal method show peaks at 1310 and 1314 eV, which are similar to that of $MgTi_2O_5$, suggesting that of Mg^{2+} ions are incorporated in octahedral sites in titania matrix. In the UV-vis absorption spectra of Mg(x)-TiO_2, the absorption edges were gradually shifted to the lower wavelength side as the amount of Mg modification increased. This result indicates the shifts of the flat band potentials of the Mg(x)-TiO_2, which contribute to the enhancement of the V_{oc}.

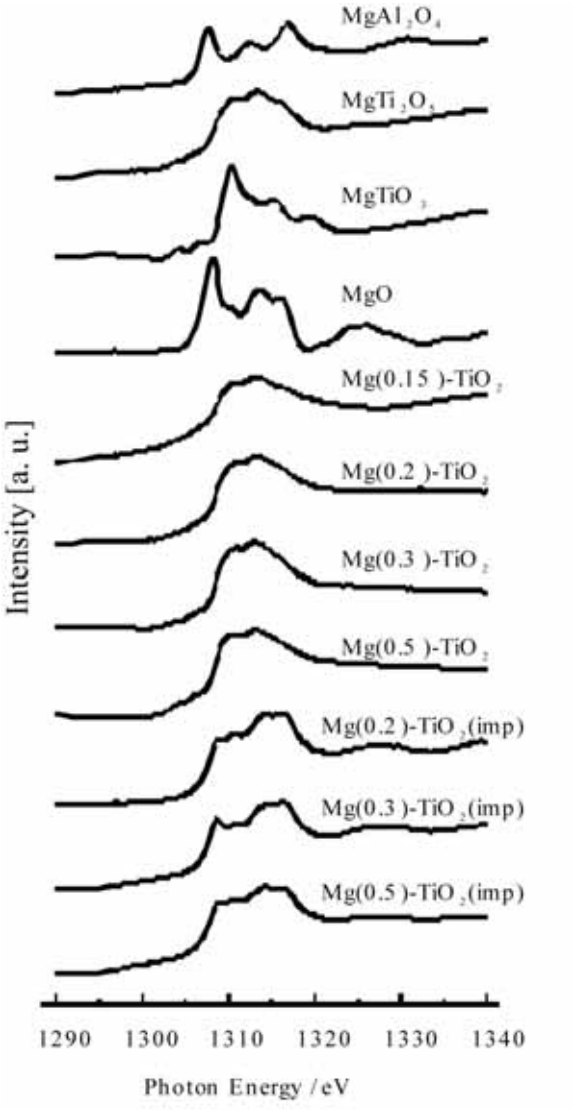

Fig. 1. Mg K-edge XANES of various Mg-containing samples.

[1] M. Grätzel, Nature **414** (2001) 338.
[2] S. Iwamoto *et al.*, ChemSusChem, in press.
[3] M. Inoue, J. Phys.: Condens. Mater **16** (2004) S1291.

BL1A

Local Environment Analysis of Mg Ions in β-Tricalcium Phosphate

K. Kawabata[1], H. Sato[1], T. Yamamoto[2]

[1]*Institute for Sports and Health Science, Kwansei Gakuin University, 662-8501 Japan*

[2]*Faculty of Science and Engineering, Waseda University, 169-8555, Japan*

Introduction

Bioactive ceramic materials, such as hydroxyapatite and β-tricalcium phosphate (β-TCP), have been widely studied and already applied in dentistry and orthopedics to repair bone defects and substitution. As it is well known that the natural bone contains many kinds of trace elements, such as Mg, Na, K, Zn, Fe, Mn etc. To understand the basic properties of natural human bone, it is very important to know the effects of these trace elements. In the present study, the local environment analysis of Mg ions in β-TCP is carried out by the near-edge X-ray absorption fine structure (NEXAFS) technique, which was successfully applied for Mn-doped β-TCP [1].

Experiments

β-TCP samples doped with Mg ions, $Ca_{2.7}Mg_{0.3}(PO_4)_2$, are synthesized by the conventional solid-state reaction method. High purity powders of $CaHPO_4$, $CaCO_3$ and $Mg(OH)_2$ were mixed and grinded in an agate mortar for an hour and the resulting powder was calcined in an air at 1273 K for 6 hours. NEXAFS measurements were carried out at BL1A in UVSOR by the total electron yield method. Powder samples were put on the carbon adhesive tape. The incident photon beams were monochromatized using double-crystal of KTP (110).

Results

Prior to the NEXAFS measurements, the sample powder was examined by using the X-ray diffraction (XRD) technique, in which no extra diffraction peaks due to the precipitates was seen in the XRD pattern. Observed NEXAFS spectrum of Mg-doped β-TCP is compared with those of the reference materials (MgO and $Mg(OH)_2$) in Fig. 1. Significant difference between these three NEXAFS spectra were clearly seen, which indicate the local environment of Mg ions in these three materials is quite different. The first principles calculations within the density functional theory (DFT) were also performed for the theoretical estimation of the NEXAFS spectra with the all-electron linearized augmented plane wave package, WIEN2k [2]. Calculated NEXAFS spectra of Mg-doped β-TCP and MgO at Mg K-edge are compared with the experimental ones in Fig. 2. Good comparison of NEXAFS spectra between observed and calculated ones can be obtained. From the results of the XRD, the NEXAFS and the first principles calculations, we could conclude that Mg ions in β-TCP are substituted on Ca^{2+} site in β-TCP. This type of combinational analysis with the NEXAFS and the first principles calculations must be applied for the analysis of local environment of other trace elements in the bioceramic materials.

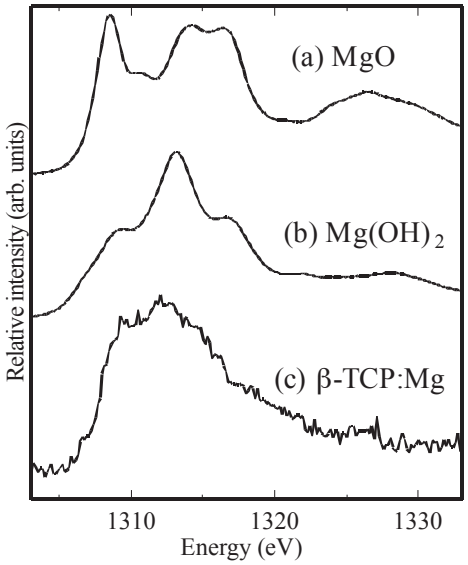

Fig. 1. Observed Mg K-edge NEXAFS spectra of (a) MgO, (b) $Mg(OH)_2$ and (c) Mg doped β-TCP.

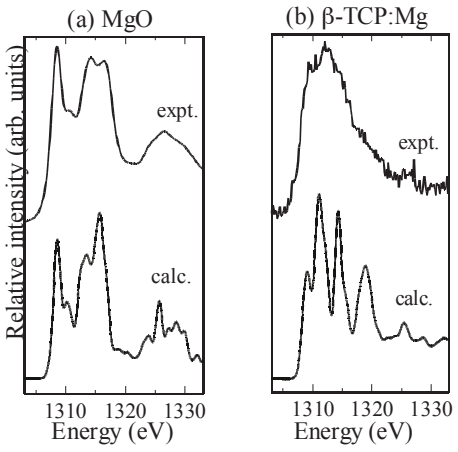

Fig. 2. Comparison between observed and calculated NEXAFS spectra at Mg K-edge of (a) MgO and (b) Mg-doped β-TCP.

[1] K. Kawabata *et al.*, J. Ceram. Soc. Jpn. **116** (2008) 108.

[2] P. Blaha *et al.*, http://www.wien2k.at.

BL1A, BL8B1

Study on the Surface Structures of the $LiNi_{0.8}Co_{0.15}Al_{0.05}O_2$ Electrode after the Preservation Tests for Li-Ion Battery Cells (II)

H. Kobayashi, M. Shikano, D. Mori

Research Institute for Ubiquitous Energy Devices, AIST, Ikeda, Osaka, 563-8577 Japan

Introduction

Several of the requirements of rechargeable batteries for hybrid electric vehicles (HEVs) are quite different to those of portable electronic devices. In particular, high specific power and long calendar life are very important requirements of HEV applications. Much effort has been applied to understanding the mechanisms that limit the calendar life of high power Li-ion cells. Until now, although the deterioration in the power performance of currently available lithium batteries is thought to result from problems with the positive electrodes, the mechanism of deterioration of the electrodes is still poorly understood. Detailed information on the changes taking place in both the cathode and anode is essential in order to determine the origin of the degradation of power performance. In this study, $LiNi_{0.8}Co_{0.15}Al_{0.05}O_2$ positive electrodes from cells that had undergone power fading through preservation tests were examined by XANES analysis to obtain information on their surfaces. The relationship between power fade and the surface state of the positive electrode was studied.

Experimental

We made 18650-type cylindrical battery cells with a capacity of about 400 mAh, which were designed to have a rate capability of more than 10 C. The positive and negative electrode was comprised of $LiNi_{0.8}Co_{0.15}Al_{0.05}O_2$ and hard carbon, respectively. Each cell was characterized using the standard battery test procedure given in the partnership for a new generation of vehicles (PNGV) Battery Test Manual. The changes in both capacity and power were checked every few weeks. After completion of the degradation test, the SOC of the cell was adjusted to 50% immediately before disassembling it, since the chemical and physical properties of the active materials are influenced by the SOC. After disassembly of the SOC-adjusted cell, the surface of the positive electrode was examined by XANES in order to study the surface film or phase transitions in particles of the active material. The Li K-edge and P-K edge XANES spectra of the samples were measured on the BL8B1 and BL1A beamline of the UVSOR Facility. Data were obtained in the total electron yield (TEY) modes.

Results

Table 1 summarizes the relative capacity and power after preservation tests. The relative capacity and power decreased on increasing the test temperature from 40 ºC to 60 ºC. Figure 1 shows the Li K-edge XANES spectra of 50% SOC samples before and after preservation tests. In TEY mode on the BL8B1, Li K-edge XANES spectra provide information on the surface structure. The spectrum measured before preservation tests contained peak A, corresponding to LiF. After the preservation tests, the intensity of peak A clearly decreased at 60 ºC after 96 weeks and the shape of peak A was close to that of the Li_2CO_3 spectrum (data not shown). These results indicate that a part of the layered structure at the surface of the positive electrode was covered with Li_2CO_3 at 60 ºC after 96 weeks. In TEY mode on the BL1A, P K-edge XANES spectra also provide information on the surface structure. The P K-edge spectrum measured before and after preservation tests showed the existence of P-containing surface films (data not shown). The relationship between power fade and the surface state of the positive electrode will be studied in detail.

Table 1. Summary of preservation test results.

Temp.	Preservation Period (Weeks)	Relative Capacity	Relative Power
40C°	96	0.918	0.868
60C°	96	0.716	0.571

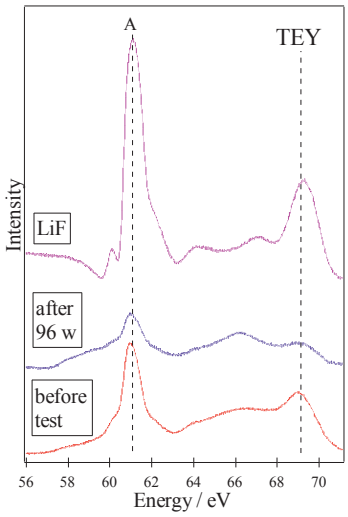

Fig. 1. Li K-edge XANES spectra for the positive electrode before and after preservation tests at 60 ºC.

BL1A

Characterization of Aluminum Naphthalocyanine Complexes by X-ray Absorption Spectra at Cl and Al K-Edges

T. Kurisaki[1], D. Tanaka[1], Y. Sakogawa[1], H. Wakita[1,2]

[1]*Department of Chemistry, Faculty of Science, Fukuoka University, Nanakuma, Jonan-ku, Fukuoka 814-0180, Japan*

[2]*Advanced Materials Institute, Fukuoka University, Nanakuma, Jonan-ku, Fukuoka 814-0180, Japan*

Naphthalocycnine (NPC) has p-conjugated system bigger than that of phthalocycnine (PC). Therefore, the metal complexes of NPC is expected a very interesting property. However, the electronic structure of naphthalocycnine is not well known. In the previous work, we studied the electronic structure of aluminum phtalocycnine by the X-ray absorption spectroscopy [1, 2]. This result suggested that there is correlation between the shape of XANES spectrum and the local structure

In this work, we applied the x-ray absorption near edge structure (XANES) spectroscopy to aluminum compounds combined with oxygen atoms. The results of the measurement indicate unoccupied and occupied electronic structure of aluminum compounds. The X-ray absorption spectra were measured at BL1A of the UVSOR in the Institute of Molecular Science, Okazaki [3]. The ring energy of the UVSOR storage ring was 750MeV and the stored current was 110-230 mA. Al K-edge absorption spectra were recorded in the regions of 1620-1750eV by use of two KTP(011) crystals. The absorption was monitored by the total electron yield using a photomultiplier. The samples were spread into the carbon tape on the first photodynode made of CuBe of the photomultiplier.

The Al K-edge XANES spectra for the aluminum naphthalocycnine and aluminum phthalocycnine are shown in Fig. 1. A change of the spectral patterns was not clearly observed between the aluminum naphthalocycnine and aluminum phthalocycnine. This result showed that the electronic structures of the aluminum ion in these complexes are about the same. We are going to try to analyze the Cl K edge XANES spectra.

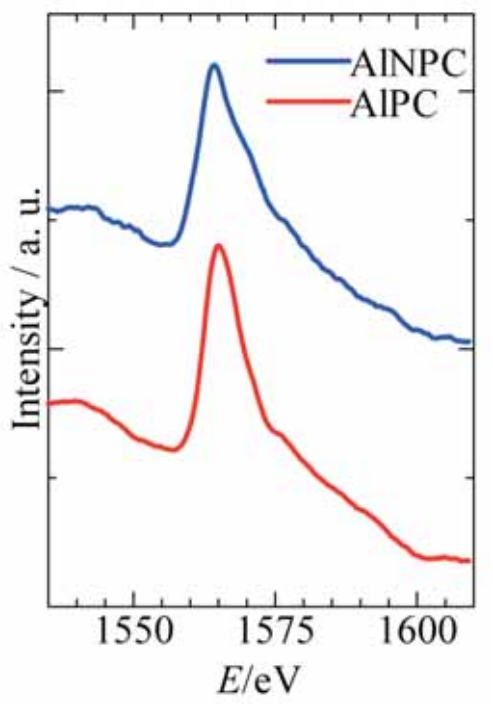

Fig. 1. Observed Al K-edge XANES spectra of aluminum naphthalocycnine and aluminum phthalocycnine

[1] H. Ichihashi *et al.*, Jpn. J. Appl. Phys. **38** *(suppl.)* (1999) 101.

[2] S. Matsuo *et al.*, Adv. Quan. Chem. **42** (2002) 407.

[3] S. Murata *et al.*, *Rev. Sci. Instrum*. **63** (1992) 1309.

BL1A

Study of Al K-Edge of Local Structure in Mesoporous Alumina Bulk Prepared by Hydrothermal Hot-Pressing

A. Nakahira, H. Nishimoto, H. Nagata, Y. Hamada, T. Kubo
Osaka Prefecture University, Gakuen-cho, Sakai 599-8531, Japan

Mesoporous alumina has attracted much attention because of their possible uses as supports for catalysts and adsorption. However, the application of mesoporous alumina was restricted because it was obtained as a powder only. Solidification of mesoporous alumina will improve handleability and expand application. Nakahira et al reported that densified bulky mesoporous silica was successfully synthesized using hydrothermal hot-pressing (HHP) method [1]. Therefore, we attemped to synthesize mesoporous alumina bulk by this HHP method and exmine the local structure around Al by XANES spectra.

Mesoporous alumina powder was prepared as a starting material [2]. Mixture of powder and water was heated at 110 °C with the uniaxial pressing under 40MPa and kept constant for 2 hours. Obtained bulks were identified by XRD. Al K-edge XANES spectra were obtained in a total electron yield mode at room temperature using a KTP double–crystal monochrometer at BL01A of the UVSOR. The spectra were collected in the photon energy range from 1520 to 1600 eV atintervals of 0.05 eV with a dwell time of 1 s.

XRD patterns showed that mesoporous alumina HHP bulk was also retained the mesoporous structure after HHP. Figure 1 shows the results of Al K-edge XANES of mesoporous alumina HHP bulk (a), starting mesoporous alumina powder (b), and γ-alumina (c) as reference materials of amorphs-like γ-alumina. The spectrum of HHP bulks was significantly similar to those of starting mesoporous alumina powder and γ-alumina. Hence, there is no apparent change in the relative intensity nor the width of these spectra. These results of XANES revealed that there is not large difference for local structure around Al between bulks prepare by HHP and ones before HHP treatment.

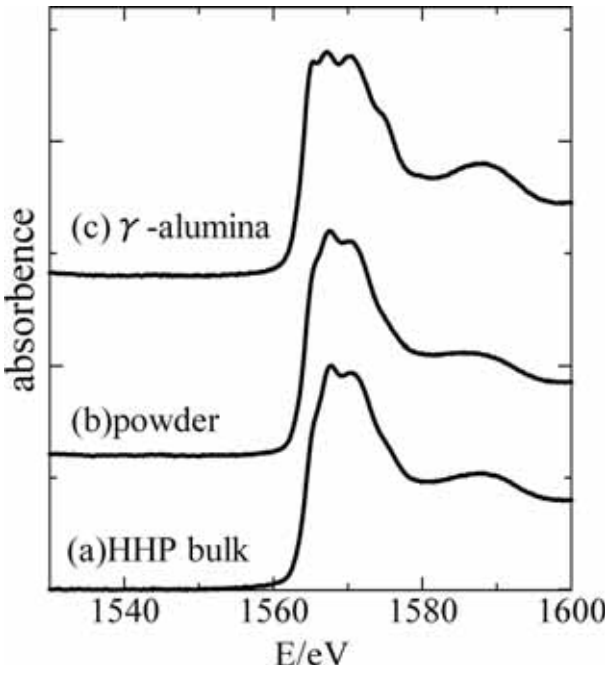

Fig. 1. Al K-edge XANES spectra of mesoporous alumina bulk prepared by HHP.

[1] H. Nagata *et al.*, Materials Transactions **47** (8) (2006) 2103.
[2] F. Vaudry, S. Khodabandeh, M. E. Davis, American Chemical Society **8** (1996) 1451.

BL1A

Structure Charactarization of Poly(vinyl butyral)-Silica Organic-Inorganic Nano-Hybrid by X-Ray Absorption Spectrum

H. Nameki[1], T. Yoshida[2], S. Yoshimoto[1], K. Yamada[1], H. Fukaya[1]

[1]*Indusrial Research Institute, Aichi Prefecture, nishi-shinwari, Kariya 448-0003, Japan*

[2]*Department of Materials, Physics and Energy Engineering, Nagoya University, Furo-cho, Chikusaku, Nagoya 464-8603, Japan*

Introduction

The organic-inorganic nano hybrids are expected as a new material that has the properties of both the inorganic materials and the organic materials. In general, flexibility and hardness are the trade-off relation, and then materials which have both the flexibility and the hardness have been difficult to prepare in past technology. By nano-level hybridization of poly(vinyl butyral) as the organic material and silica(SiO_2) as the inorganic material, we developed a novel material that has both flexibility(impact resistance) and hardness simultaneously[1]. To consider the appearance mechanism of this peculiar property, we examined the structure of the hybrid by X-ray absorption spectroscopy.

Experimental

Alkoxides(tetraethoxysilane and 3-glycidoxy-propyltrimethoxysilane) were added into 5% 2-propanol solution of PVB, and HCl or NH_4OH was added into the mixture as catalyst(the amount of the catalyst is 0.05mol per 1 mol of total alkoxides). In a part of these sample, water(10mol per 1mol of total alkoxides) was added to reacting solution. Thus, sample preparation was done by four methods(shown in table1). The reacted solution was stirred for 2 hours further, and then this was coated into a brass substrate. The coated substrate was preserved in a desiccator for 16 hours, and then heated first at 333K for 2h, next at 363K for 2h. Structure characterization of these sample was done by measuring Si-K edge X-ray absorption spectra at BL1A in UVSOR.

Results and Discussion

Figure 1 shows X-ray absorption spectra of samples and a silica glass as standard material. In all spectra, peak of strong intensity was observed at 1845eV, which was assigned to Si-K edge absorption. Above the energy of the peak, oscillation pattern due to the structure around Si atom was observed.

The oscillation pattern of sample #2 and that of sample #4 were quite similar to each other, on the other hand, these were different from that of sample #1 or #3. Sample #2 and 4 were prepared through H_2O addition, then hydrolysis of alkoxides was occurred and alkoxides was polymerized to form silica(SiO_2 multi-units). The oscillation pattern of spectra was considered to reflect the structure of multi-units silica.

In the sample #1 or #3, alkoxides was mainly reacted with hydroxyl group of PVB, not with each other, because of no addition of H_2O. Then in sample #1 and #3, silica was dispersed as SiO_2 mono unit in the hybrid. This means the arrangement of atoms(oxygen) around Si is irregular in bond distance in sample #1 or #3. Especially, spectrum of the sample #1 was quite similar to the silica glass, which has amorphous structure.

The sample #1 is superior in the properties of transparency, flexibility and impact resistance to the sample #2,#3,#4. The structural difference showed in X-ray absorption spectra is considered to be concerned with the difference in these properties, and that may contributes the appearance of the peculiar property of sample #1.

Table 1. Sample preparation conditions.

No.	Catalyst	H_2O addition	Remarks
#1	HCl	none	showing excellent properties
#2	HCl	added	
#3	NH_4OH	none	not homogeneous sample(opaque)
#4	NH_4OH	added	not homogeneous sample(opaque)

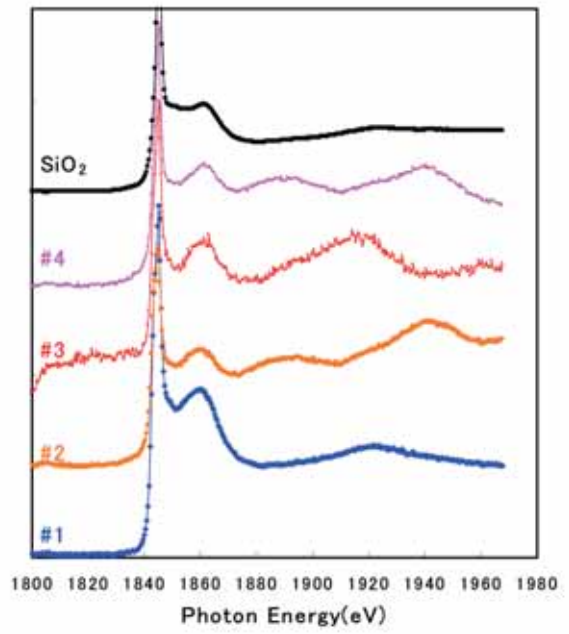

Fig. 1. X-ray absorption spectra of the hybrid samples.

[1] Japan Patent, 2007-119635.

BL1A

In-Situ Measurement of X-Ray Excited Optical Luminescence from a Silica

T. Yoshida[1], T. Tanabe[2], S. Muto[1], H. Yoshida[3]

[1]*Department of Materials, Physics and Energy Engineering, Nagoya University, Furo-cho, Chikusa-ku, Nagoya 464-8603*

[2]*Department of Advanced Energy Engineering Science, Interdisciplinary Graduate School of Engineering Science,Kyushu University6-10-1, Hakozaki, Higashi-ku, Fukuoka 812-8581*

[3]*EcoTopia Science Institute, Nagoya University, Furo-cho, Chikusa-ku, Nagoya 464-8603*

Degradation of optical properties of silica glass by ionizing radiation is one of the main concerns for their use in fusion and fission environments. Although the radiation damage of silica glass has been extensively studied, the detailed damaging processes and/or radiation effects are not yet fully understood. This is partly because most of the studies have been done by post-irradiation tests, which cannot give information on the "processes" but only "traces" or "results" since the relaxation time of excited electrons is usually very short.

Recently, we have tried *in situ* measurement of X-ray excited optical luminescence (XEOL) from a silica glass. The *in situ* measurements were very effective for observing the dynamic changes in their electrical properties by ionizing radiations. In the present study, we examined the changes in XEOL of a silica glass with respect to excitation X-ray energy near the threshold of the Si *K*-edge, irradiation time and temperature.

The sample used in this study was a low-OH fused silica glass (T-2030) disc produced by Toshiba Ceramics, Japan. The diameter and thickness of the sample were 13 mm and 2 mm, respectively. XEOL of the silica glass by X-ray energy between 1.8 and 1.9 keV was measured between 50 K and 300 K on the beam line 1A at UVSOR-II, Institute for Molecular Science. The luminescence was collected and guided by a lens in a UHV chamber to the monochromator (CP-200, JOBIN YVON) and detected by a multi-channel analyser (OMAIII, EG&G PRINCETON APPLIED RESEARCH), which covers the photon energies from ca. 1.5 eV to 4 eV.

We selected three excitation X-ray energies of 1834 eV (just below the Si *K*-edge), 1848 eV (on the white line) and 1858 eV (well above the threshold). In the measurement of XEOL at room temperature, an intense emission band peaked around 3.1 eV is observed in each spectrum. The previous studies assigned the origin of the 3.1 eV band to the intrinsic $B_{2\beta}$ center [1,2]. We also measured XEOL at lower temperatures, and found the broadening of the emission band below 100 K. Fig. 1(a) shows XEOL of the same sample measured at 50 K. A peak position is shifted to the lower energy side, because an additional emission band appears around 2.6 eV, revealed by the peak fit, as shown in Fig.1.

Figs. 1(b) shows the time evolutions of the XEOL intensities at 50 K for the three excitation energies. The intensity value of each point was evaluated by the total area of the emission band in Fig. 1(a). The luminescence intensity is monotonically decreased with the irradiation time at the excitation energy of 1848 eV, whereas at 1834 eV and 1858 eV, the intensities are nearly constant with the irradiation time. A difference spectrum (not shown) between the spectra after irradiated for 300 and 5000 seconds at 1848 eV was dominated by the component peaked at 2.6 eV, indicating that the observed intensity reduction is mainly ascribed to the reduction of this component. These results above suggest that a specific type of point defects in the sample is preferentially decomposed by a specific electronic transition excitation. In other words, a selective electronic excitation can control formation and/or annihilation of a specific type of defects.

In the present case, the transition induced by 1848 eV X-ray corresponds to that from the Si 1*s* occupied state to the 3*p* antibonding orbitals relating to the Si–O bonds. The high-density electron excitation will break the Si–O bonds and also excite the electrons trapped at the luminescent centers of the 2.6 eV band, which could effectively contribute to the decomposition of the centers.

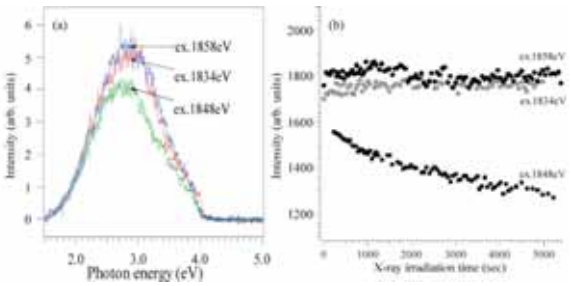

Fig. 1. (a) Optical luminescence spectra of a fused silica glass excited by X-rays with the energies of 1834, 1848 and 1858 eV at 50K. (b) Irradiation time dependence of XEOL intensities at 50 K.

[1] R. Tohmon *et al.*, Phys. Rev. B **55** (1989) 1337.
[2] S. Agnello *et al.*, J. Non-cryst. Solids **232-234** (1998) 323.

BL3U

Direct Observation of Electronic States at Inner Pentacene Thin Films Beneath Au Electrodes

H. S. Kato[1], F. Yamaguchi[1,2], M. Kawai[1,2], T. Hatsui[3], M. Nagasaka[3], N. Kosugi[3]
[1]*RIKEN (The Institute of Physical and Chemical Research), Wako 351-0198, Japan*
[2]*Department of Advanced Materials Science, University of Tokyo, Kashiwa 277-8501, Japan*
[3]*UVSOR Facility, Institute for Molecular Science, Okazaki 444-8585, Japan*

Introduction

In order to extend new functionality of electronic devices, the molecular devices have recently been investigated with great efforts. The organic field effect transistor (OFET) is a typical molecular device that controls electric conductivity by injection of carriers into the organic thin film under the applied electric field. The conductive mechanism has generally been understood with a scheme of band bending of electronic states, based on the knowledge of inorganic semiconductor transistors. However, the energy diagram might be not exactly the same between organic and inorganic materials, because of more localized orbitals of the organics. Moreover, it is also important to elucidate the difference of electronic states for future advanced devices utilizing the noble characters of organic materials. Therefore, the direct observation of electronic states in the organic thin films under operation conditions has been required.

In this study, we aim to establish a new experimental method that elucidates the electronic state change in organic thin films of OFET under the electric field. The fluorescence-yield X-ray absorption spectroscopy (FY-XAS) should be a promising method for detection of inner electronic states of organic devices, because the fluoresced X-ray has a long mean free path more than several 10 nm in most of materials even for soft X-ray excitation. In addition, the X-ray is not disturbed by applied electric field, besides emitted electrons. Thus, we have attempted to utilize FY-XAS for investigation of inner electronic states of OFETs.

Experimental

To investigate the electronic states of OFET, pentacene (Pn) thin films on the SiO_2-covered Si substrates were fabricated using a molecular beam deposition system at RIKEN. The quality of their morphology and crystallinity was high enough in comparison with those in previous reports. The performance for FETs of the fabricated Pn thin films was also confirmed with additive deposition of Au electrodes on the films. By the same preparation, the fully Au-covered Pn thin-film samples were made to evaluate the field effects obtained from uniform electric fields in the films.

The FY-XAS measurements were performed at the BL3U beamline of UVSOR facility in IMS. The samples were set in a BL3U end-station through sample-entry system. The fluorescence intensities were measured using a retarding field detector consisting of MCP plates.

Results and Discussion

Figure 1 shows the incidence angle dependence of fluorescence-yield C K-edge XA spectra of the Pn films (t = 20 nm), in which the spectra of a non Au-covered Pn film and a fully Au-covered Pn film are compared. In both cases, the relative intensities of π^* components at photon energies of ≈ 285 eV decrease with increasing incidence angle of excitation X-ray, while the broad σ^* components above 300 eV increase with increasing incidence angle. These results are consistent with the structure of crystallized Pn thin films on SiO_2 substrates; the molecular axis is towards surface normal with a small tilting angle in each monolayer. The small difference between the non Au-covered and fully Au-covered Pn films would be due to a perturbation at the Au deposition form a thermal evaporation source. However, the similarity in the incidence angle dependence of the spectra evidences that the perturbation is not significant for the whole Pn thin film. As above, the FY-XAS measurements have enough potential to characterize the inner organic thin films even beneath electrodes.

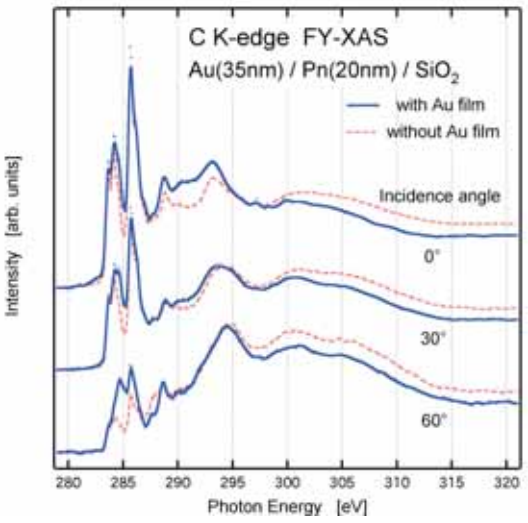

Fig. 1. Incidence angle dependence of fluorescence yield C K-edge XA spectra of pentacene thin films on SiO_2-covered Si substrate, in which the spectra of a non Au-covered Pn film (red broken lines) and a fully Au-covered Pn film (blue solid lines) are compared. The incidence angle is defined from surface normal.

BL4B

Study on the Surface Structures of the $LiNi_{0.8}Co_{0.15}Al_{0.05}O_2$ Electrode after the Preservation Tests for Li-Ion Battery Cells (I)

H. Kobayashi, M. Shikano

Research Institute for Ubiquitous Energy Devices, AIST, Ikeda, Osaka, 563-8577 Japan

Several of the requirements of rechargeable batteries for hybrid electric vehicles (HEVs) are quite different to those of portable electronic devices. In particular, high specific power and long calendar life are very important requirements of HEV applications. Much effort has been applied to understanding the mechanisms that limit the calendar life of high power Li-ion cells. Until now, although the deterioration in the power performance of currently available lithium batteries is thought to result from problems with the positive electrodes, the mechanism of deterioration of the electrodes is still poorly understood. Detailed information on the changes taking place in both the cathode and anode is essential in order to determine the origin of the degradation of power performance. In this study, $LiNi_{0.8}Co_{0.15}Al_{0.05}O_2$ positive electrodes from cells that had undergone power fading through preservation tests were examined by XANES analysis to obtain information on their surfaces. The relationship between power fade and the surface state of the positive electrode was studied.

Experimental

We made 18650-type cylindrical battery cells with a capacity of about 400 mAh, which were designed to have a rate capability of more than 10 C. The positive and negative electrode was comprised of $LiNi_{0.8}Co_{0.15}Al_{0.05}O_2$ and hard carbon, respectively. Each cell was characterized using the standard battery test procedure given in the partnership for a new generation of vehicles (PNGV) Battery Test Manual. The changes in both capacity and power were checked every few weeks. After completion of the degradation test, the SOC of the cell was adjusted to 50% immediately before disassembling it, since the chemical and physical properties of the active materials are influenced by the SOC. After disassembly of the SOC-adjusted cell, the surface of the positive electrode was examined by XANES in order to study the surface film or phase transitions in particles of the active material. The O K-edge XANES spectra of the samples were measured on the BL4B beamline of the UVSOR Facility. Data were obtained in the total electron yield (TEY) mode.

Results

Figure 1 shows the preservation period vs. relative capacity and power. The relative capacity and power decreased on increasing the test temperature from 40 ºC to 60 ºC. Figure 2 shows the O K-edge XANES spectra of 50% SOC samples before and after preservation tests. In TEY mode, O K-edge XANES spectra provide information on the surface structure. The spectrum measured before preservation tests contained peak A, corresponding to oxygen originating from the layered structure, and peaks B and C. After the preservation tests, the intensity of peak A clearly decreased at 60 ºC after 96 weeks, while the intensities of peaks B and C increased. The position of peak B was close to that of the NiO spectrum, indicating the existence of a cubic phase on the surface, and the position of peak C was close to that of Li_2CO_3, or to conductive materials such as AB (data not shown). These results indicate that a part of the layered structure at the surface of the positive electrode was transformed to a cubic structure at 60 ºC after 96 weeks.

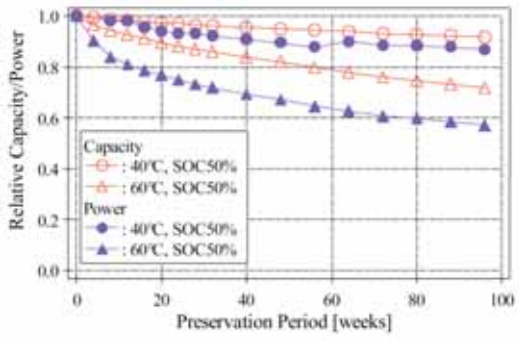

Fig. 1. Preservation period vs. relative capacity and power.

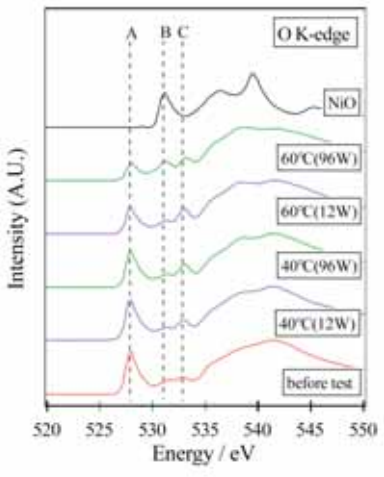

Fig. 2. O K-edge XANES spectra for the positive electrode after preservation tests at 40 ºC and 60 ºC.

BL4B

Magnetic Properties of C_{60} and Co Nanocomposite Films

Y. Matsumoto[1], S. Sakai[1], T. Takagi[2], T. Nakagawa[2], T. Yokoyama[2]

[1]*Advanced Science Research Center, Japan Atomic Energy Agency (JAEA), Tokai Naka-gun, Ibaraki 319-1195 Japan*

[2]*Department of Materials Molecular Science, Institute of Molecular Science (IMS), Okazaki, Aichi 444-8585, Japan*

Recently, we have found that fullerene (C_{60}) and cobalt (Co) nanocomposite films show large tunnel magnetoresistance (TMR) effects at low temperature [1]. As shown schematically in a figure 1, these films consist of a matrix of C_{60}-Co compounds and dispersed Co nano particles [2]. However, observed TMR effects cannot be explained only by a spin transport among the Co particles even if they are completely spin polarized. Therefore, in the present work, we have investigated local magnetic properties of C_{60}-Co films by X-ray magnetic circular dichroism (XMCD) spectroscopy.

MCD measurements were performed at beam line 4B with a super conducting magnet. The details of this MCD system are described elsewhere [3]. Different Co content films of $C_{60}Co_x$ (x: the number of Co atoms per a C_{60} molecule) were prepared by a co-deposition method [1] under the UHV condition ($<10^{-7}$Pa) and then transferred into the experimental chamber without breaking the vacuum. The Co $L_{III,II}$-edge MCD spectra were taken with the polarization factor of ~0.85. Total energy resolution of 0.75eV was applied in the present work.

Figure 2(a) and 2(b) show XAS spectra at the Co 3d←2p excitation, and MCD spectra of different contents of $C_{60}Co_x$ and pure-Co films measured at 5T and 4.9K, respectively. In the case of Co dense films (x>10), peak profiles of MCD spectra are similar to those of the pure Co film. This result indicates that Co particles dispersed into the film have a same magnetic property as a Co metal. On the other hand, in the case of Co dilute films (x<10), MCD signal are different to pure-Co film (see inset, Fig. 2(b)). According to our previous works of Raman spectroscopy [2], the matrix of C_{60}-Co compounds is dominant in this composition domain. In fact, XAS spectrum of $C_{60}Co_{4.3}$ has several fine structures as shown in Fig. 2(a) in contrast to the Co film. Though the derails of such structures which show MCD responses are not clearly right now, it is expected that they are connected to the hybrid molecular orbitals (MOs) of Co 3d band and C_{60} π^* orbital from XPS and C K-edge NEAXFS measurements. In addition, it has been also observed that MCD signal of Co dilute films indicate the strongly temperature dependence (not shown in figures here). Especially, MCD signal of $C_{60}Co_{4.3}$ film was vanished at 77K. These findings indicate that there are hybrid MOs which show paramagnetic properties in the C_{60}-Co compounds. It is speculated that these states act as a spin-filter in spin transport processes.

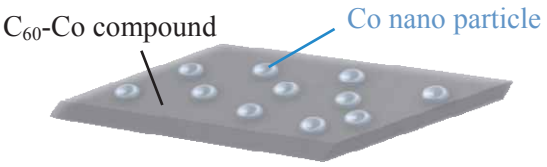

Fig. 1. Schematically illustration of the C_{60} and Co nanocomposite film.

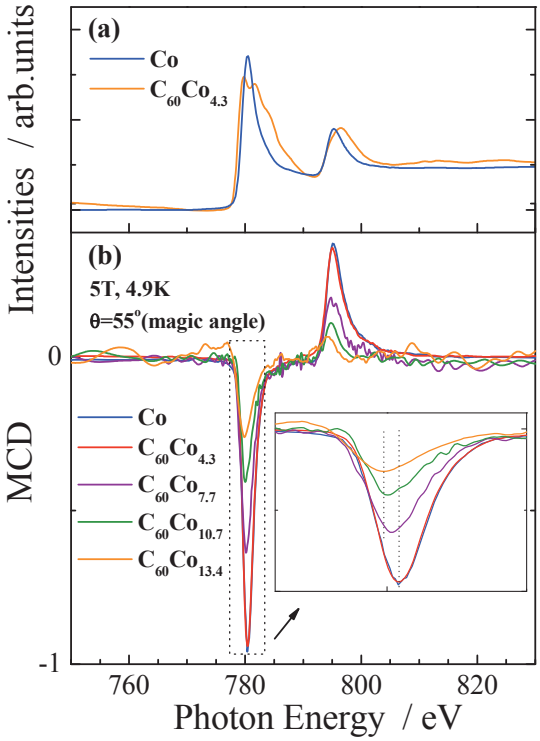

Fig. 2. Co L-edge XAS spectra (a), and MCD spectra of different Co contents of $C_{60}Co_x$ and the pure Co -film measured at 5T and 4.9K (b).

[1] S. Sakai, I. Sugai, S. Mitani, K. Takanashi, Y. Matsumoto, H. Naramoto, P. V. Avramov, S. Okayasu, Y. Maeda, Appl. Phys. Lett. **91** (2007) 242104.

[2] S. Sakai, H. Naramoto, V. Lavrentiev, K. Narumi, M. Maekawa, A. Kawasuso, T. Yaita, Y. Baba, Mater. Trans. **46** (2005) 765.

[3] T. Nakagawa, T. Takagi, Y. Matsumoto, T. Yokoyama, Jpn. J. Appl. Phys. *in press*.

BL5U

Valence Band Spectra of Fe/Si Interfaces Changing Probing-Depth

T. Ejima, T. Goto, T. Jinno

Institute for Multidisciplinary Research for Advanced Materials, Tohoku University, Sendai 980-8577 Japan

Node and antinode positions of standing waves can easily move in uppermost layers of the multilayer, therefore photoelectrons excited in the uppermost layers can be effectively scanned through the interface of the layers [1]. Recently, these positions can be determined by total electron yield (TEY) spectra measured simultaneously with reflection spectra [2].

Magnetic coupling between Fe layers in Fe/Si multilayers exhibits initially ferromagnetic one, then antiferromagnetic, and finally ferromagnetic or no coupling with an increase of the sandwiched Si layer thickness [3]. When the thickness of the Si layer is 2.0 – 2.5 nm, the coupling changes from antiferromagnetic one to ferromagnetic or non-magnetic one. The origin of this inter-layer coupling is controversial, and is roughly classified into either a metallic model as Fe-Si compound or a semiconductor model as amorphous Si [4, 5]

In this study, electronic structures of Fe/Si interfaces of Fe/Si/Fe trilayers deposited on a Mo/Si reflection multilayer are investigated using photoelectron spectroscopy changing the probing depth, which is caused by the phase changes according to the changes of the thicknesses of the uppermost trilayers and of incident wavelength. The phase changes are observed in situ by both TEY and reflection spectra.

Nominal layer structure of the Fe/Si/Fe trilayer estimated from the experimental deposition rates is represented in Fig. 1. Magnetic behavior of this trilayer estimated from the VSM measurement was ferromagnetic one. The photoelectron spectra were measured with TEY spectra. Probing depth estimated from the TEY and reflection spectra is represented in Fig. 1 concerning with the Ar^+ etching time and obtained UPS spectra [2].

Obtained UPS spectra represented in Fig. 2 can be classified into 3 groups: first is a Fe-Si compound structure (spectra b – d), second is an amorphous Si structure (spectra e – f), and the last is a Fe structure (spectra h & i). This classification of the electronic structures suggests that inter-diffusion layer between Fe/Si layers is formed when a Fe layer is deposited onto a Si layer, and not formed when a Si layer is deposited onto a Fe layer. The second Si-like electronic structures observed between the Fe layers suggest that the origin of the coupling is well explained by the semiconductor model, if the ferromagnetic behavior is caused by the inter-layer coupling.

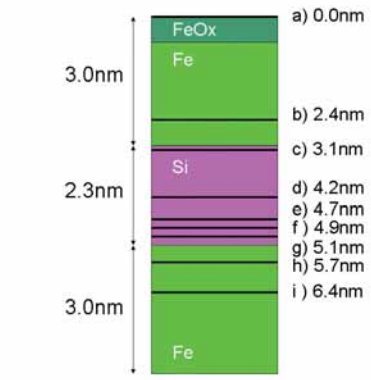

Fig. 1. Nominal layer structure of Fe/Si/Fe trilayer with estimated probing depth.

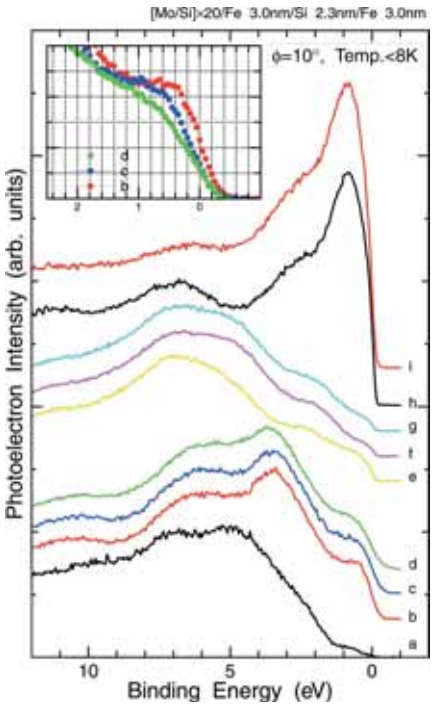

Fig. 2. Valence band spectra of Fe/Si interfaces changing the probing depth. Characters represent the probing depths that are designated in Fig. 1.

[1] S. –H. Yang *et al.*, J. Phys., Condens. Matter **14** (2002) L407.
[2] T. Ejima *et al.*, Appl. Phys. Lett. **89** (2006) 021914.
[3] E. E. Fullerton *et al.*, J. Magn. Magn. Mater. **117** (1992) L301.
[4] For example, P. Bruno, C. Chappert, Phys. Rev. Lett. **67** (1991) 1602.
[5] For example, D. M. Edwards *et al.*, Phys. Rev. Lett. **67** (1991) 493.

BL5U

Fermi Surface Mapping of 8 ML Fe/Cu(001) by Angle-Resolved Ultraviolet Photoemission Spectroscopy

X. Gao[1], H. Miyazaki[2,3], S. Chen[1], A. T. S. Wee[1], T. Ito[3], S. Kimura[3], J. Yuhara[2], K. Soda[2,3]

[1]*Department of Physics, National University of Singapore, Singapore 117542*

[2]*Graduate School of Engineering, Nagoya University, Nagoya 464-8603, Japan*

[3]*UVSOR Facility, Institute for Molecular Science, Okazaki 444-8585, Japan*

Introduction

Despite many years' research efforts in Fe/Cu(001) system, it remains one of the most complicated magnetic thin film systems. It is generally believed that there are three thickness range of the Fe film with different magnetic properties and structures [1]: below 3 monolayers (ML), Fe film has so-called face center distorted (fct) structure and is ferromagnetic; from 4 ML to about 10 ML, the film has a ferromagnetic fct top layer with the rest layers either anti-ferromagnetic or paramagnetic with fcc structure depending on the temperature; above 11 ML, the whole film changes to bcc structure and is ferromagnetic. Non-uniform reduced magnetic response in the second thickness range than in the other two ranges are still full of mysteries and there are still disputes about its nature. Fermi surface mapping by ultraviolet photoemission spectroscopy (UPS) is a powerful technique to study electronic structure in k space. Although there have been Fermi surface mapping studies of Co and Ni grown on Cu(001) and many studies of valence band using UPS for Fe/Cu(001), no Fermi surface mapping has been reported so far for Fe/Cu(001).

Experimental

Cu(001) surfaces were prepared by cycles of Ar^+ ion bombardment at 1 keV and annealing at 800 K in an ultrahigh vacuum system. The (1x1) pattern was clearly observed on the clean Cu (001) surface by low energy electron diffraction. 8 ML Fe film was *in situ* evaporated onto the Cu(001) surface at room temperature, which was cooled down to 5 K for UPS. The thickness was monitored by a quartz oscillator and calibrated using XPS. Angle-resolved photoelectron spectra were recorded under 2.7 x 10^{-8} Pa with a high-resolution energy analyzer at BL5U. The total energy resolution was 14 meV with the excitation photon energy of 90 eV at 5 K.

Results and Discussion

Figure 1 shows the photoemission intensity of 8 ML Fe/Cu(001) along [001] direction recorded at a photon energy of 90 eV. Dispersions of both Fe 3*d* at the Fermi surface and Cu 3*d* at the binding energy of about 2 eV can be clearly observed.

Figure 2 shows Fermi surface mapping for 8 ML Fe/Cu(001) at 5 K obtained from angle-resolved UPS using the photon energy of 90 eV. The energy slice for the mapping is set at the binding energy of 0.4 eV. Further study of the Fermi surface mapping using different photon energies at various temperatures to compare with theoretical calculation should help to understand the nature of the fcc Fe films on Cu(001).

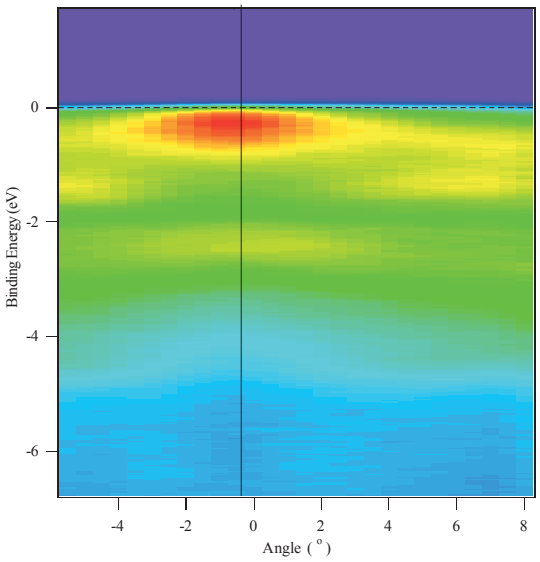

Fig. 1. Photoemission intensity of 8 ML Fe/Cu(001) around [001] direction (indicated by the dark solid line).

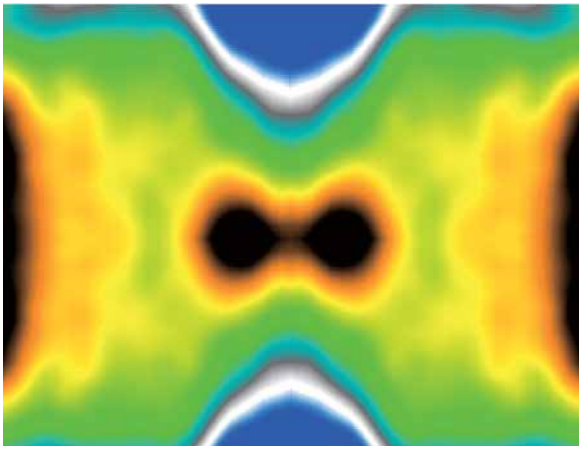

Fig. 2. Fermi surface mapping for 8 ML Fe/Cu(001) at 5 K using photon energy of 90 eV.

[1] D. Li *et al.*, Phys. Rev. Lett. **72** (1994) 3112; D. Li *et al.*, Appl. Phys. **76** (1994) 6425.

BL5U

Ce and Gd 4d-4f Resonant Photoemission Studies of $Ce_{1-x}Gd_xCoSi_3$

H.J. Im[1,2], H. Miyazaki[3,2], T. Ito[2,4], S. Kimura[2,4], J.B. Hong[1], Y.S. Kwon[1]
[1]*Department of Physics, Sungkyunkwan University, Suwon 440-746, Korea*
[2]*UVSOR Facility, Institute for Molecular Science, Okazaki 444-8585, Japan*
[3]*Graduate School of Engineering, Nagoya University, Nagoya 464-8603, Japan*
[4]*School of Physical Sciences, The Graduate University for Advanced Studies, Okazaki 444-8585, Japan*

We have performed Ce and Ge 4d-4f resonant photoemission spectroscopy (RPES) on $Ce_{1-x}Gd_xCoSi_3$ systems in order to understand the origin of quantum criticality in view of electronic structure. As Gd is replaced by Ce, the ground state changes from the antiferromagnetic (x = 1.0, 0.8, 0,6) to non-magnetic heavy fermion (x = 0, 0.2) via the quantum critical point (QCP, x = 0.4) [1,2]. This is considered as a new type of QCP since the antiferro-magnetism and non-magnetism originate from the different kinds of f-electrons belonging to Gd and Ce ions, respectively, and seem to compete each other causing the QCP. Therefore, the studies of the electronic structure of both Gd and Ce 4f states are essential to understand the new QCP [1,2].

RPES measurements for polycrystalline samples $Ce_{1-x}Gd_xCoSi_3$ (x = 0, 0.2, 0.4, 0.6, 1) were carried out at BL5U. The used photon energies are 120 (on) and 113 eV (off) for Ce 4d-4f RPES, and 146.5 (on) and 134.8 eV (off) for Gd 4d-4f RPES. Total energy resolutions are about 65 and 95 meV for the photon energies of 120 and 146.5 eV, respectively. Measurement temperature is 10 K. Sample surfaces were prepared by *in situ* fracturing under 2×10^{-8} Pa. Sample cleanliness is checked by the absence of oxidization peak around 6 and 10 eV.

Figure 1 displays Gd 4d-4f on-RPES spectra for x = 0.2, 0.4, 0.6, and 1. All spectra are subtracted by Shirley background, and then are normalized to the intensity of Gd $4f^6$ final-state peaks around -8.4 eV according to the Gd composition ratio. In the regime of from -3.5 to -2 eV, the broad peaks, which are overlap of both Ce $4f^0$ final state and non-f-states, are observed. Particularly, the Ce $4f^1$ final-states, the so-called tail of Kondo resonance, show some variation. For the meaningful comparison of Kondo resonance peaks, Ce 4f spectra should be extracted, precisely.

Figure 2 shows the Ce 4f spectra for x = 0, 0.2, 0.4, and 0.6, which are obtained by the subtraction of off-spectra from on-spectra in Ce 4d-4f RPES. We clearly observe the well-defined Ce $4f^0$ and Ce $4f^1$ final states around -2.5 eV and at the Fermi level, respectively. It should be noted that the sharp tail of Kondo resonance (Ce $4f^1$-state near E_F) persists from non-magnetic (x = 0, 0.2) to magnetic (x = 0.6) regime via the QCP (x = 0). This indicates that the new kind of QCP in this system does not come from the change of Ce 4f electronic structures unlike a local quantum critical scenario [5].

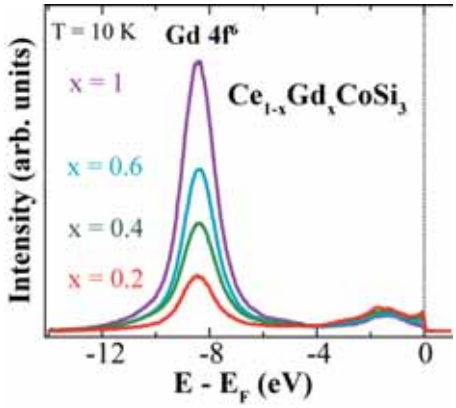

Fig. 1. Gd 4d-4f on-RPES spectra of $Ce_{1-x}Gd_xCoSi_3$.

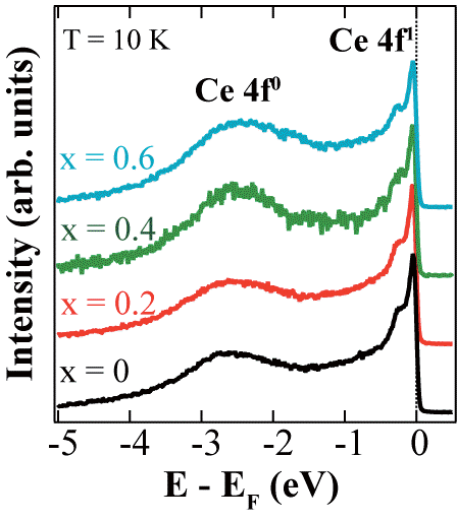

Fig. 2. Ce 4f spectra of $Ce_{1-x}Gd_xCoSi_3$ obtained in Ce 4d-4f RPES measurements.

[1] J.B. Hong *et al.*, J. Magn. Magn. Mater. **310** (2007) 292.
[2] J.B. Hong *et al.*, Physica B **403** (2008) 911.
[3] D. Eom *et al.*, J. Phys. Soc. Jpn. **67** (1998) 2495.
[4] H.J. Im *et al.*, Phys. Rev. B **72** (2005) 220405.
[5] Q. Si *et al.*, Nature **413** (2001) 804.

BL5U

Photoemission Studies on Quantum-Well States of Pb-Covered Ag Films on Si(111)

H. Ke, H. Narita, I. Matsuda
Institute for Solid State Physics (ISSP), University of Tokyo, 5-1-5 Kashiwanoha, Chiba 277-8581, Japan

Spin controls in utrathin metal films have been important topics in developing (nanometer-scale) spintronics and studying modern solid state physics. When thickness of metal film reduces to electron wavelength, electron energy is quantized by quantum size effect, resulting in formation of quantum-well states (QWS's). In contrast to isolated metal thin films, those on solid substrates have shown new intriguing spin properties through boundary conditions between films and substrates.[1] Spin-polarization of quantum Ag film has been reported when the film was grown on Fe substrate (*e.g.* Fe).[2] The polarization originates from spin-polarized bulk bands of the ferromagnetic metal substrate, which induces spin-dependent reflection phase shift at the film/substrate interface for electrons confined in the film. While varieties of spin properties have been reported in nanometer-thick metal film on metal substrates, there has been little report for those on the semiconductor substrates.

In the present research, we have challenged to realize spin-split bands in a nonmagnetic metal (Ag) film on a semiconductor (Si) substrate by ultilizing the strong Rashba effect at a surface atomic layer induced by heavy metal deposition. Up to now, we have succeeded in demonstrating spin-splitting of QWS subbands for Bi-covered quantum Ag film on Si(111).[3] Then, we move on to Pb-covered Ag film on Si(111). In contrast to the former case, the latter one is expected show spin-split Fermi surfaces, which induce exotic macroscopic properties.

The experiment was performed at the undulator beamline of BL-5U at UVSOR. With a high-resolution analyzer of MBS-Toyama 'Peter' A-1, angle-resolved photoemission spectroscopy measurements were performed at photon energy of 21 ~ 29 eV.

Figure (a) shows experimental band dispersion of thin Ag film (~30 ML) deposited on Si(111)7x7. We observed clear Fermi-edge and a broad spectra feature around 2 eV. On the other hand, after 1 ML-Pb adsorption on the Ag film, we detected subbands of QWS as shown in Fig. (b). This drastic spectral change is likely due to change of the film morphology. The Pb adatoms seemed to induce formation of continuous Ag film from rough Ag islands on Si(111). Analyses of the band parameters are underway.

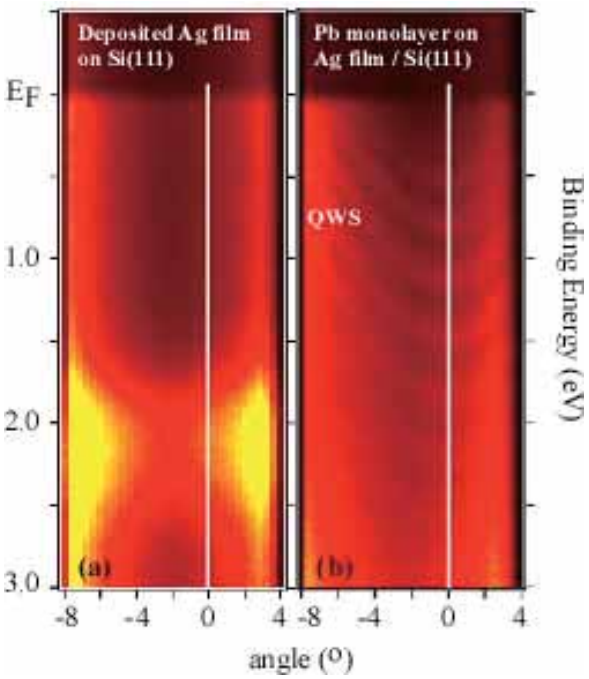

Fig. 1. Experimental band dispersion diagrams for (a) ~30 ML-Ag film deposited on Si(111)7x7 and (b) that is subsequently covered with Pb monolayer.

[1]*(A review paper)* I. Matsuda *et al.*, e-J. of Surf. Sci. and Nanotechnology **2** (2004) 169.
[2] N. V. Smith *et al.*, Phys. Rev. B **49** (1994) 332.
[3] H. Ke *et al.*, submitted to Phys. Rev. Lett.

BL5U

Temperature-Dependent Angle-Resolved Photoemission Spectra on Ferromagnetic EuO Thin Films

H. Miyazaki[1,2], T. Ito[2,3], S. Ota[1,2], H. J. Im[4], S. Yagi[1], M. Kato[1], K. Soda[1,2], S. Kimura[2,3]

[1]*Graduate School of Engineering, Nagoya University, Nagoya 464-8603, Japan*

[2]*UVSOR Facility, Institute for Molecular Science, Okazaki 444-8585, Japan*

[3]*School of Physical Sciences, The Graduate University for Advanced Studies, Okazaki 444-8585, Japan*

[4]*Department of Physics, Sungkyunkwan University, Suwon 440-746, Korea*

Europium monoxide (EuO) is a ferromagnetic semiconductor with the Curié temperature (T_C) at around 70 K [1, 2]. In the electron doping case by the Eu excess or substitute Gd^{3+} or La^{3+} from Eu^{2+} ion, the T_C increases up to 150 K and the electrical resistivity drops twelve-order of magnitude below the T_C originating in a metal-insulator transition (MIT) [2, 3]. To reveal the origin of these physical properties of EuO, it is important to clarify the electronic structure. Three dimensional angle-resolved photoemission spectroscopy (3D-ARPES) using a synchrotron radiation source is the most powerful technique to directly determine the electronic band structure. Using this technique we observed the change in the Eu 4*f* and O 2*p* states across T_C.

Single-crystalline EuO thin films with a thickness of about 50 nm were fabricated by the molecular beam epitaxy (MBE). Epitaxial growth of the single-crystalline EuO thin films with the 1 x 1 EuO (100) patterns was confirmed with low energy electron diffraction (LEED) and reflection high energy electron diffraction (RHEED) methods. The T_C measured with a superconducting quantum interference device (SQUID) magnetometer was 71 K. The 3D-ARPES measurements were performed at the beam line 5U of UVSOR-II combined with the MBE system. The total energy and momentum resolutions for the ARPES measurement were set 123 meV and 0.020 $Å^{-1}$ at the Γ point and 45 meV and 0.014 $Å^{-1}$ at the X point, respectively.

Figure 1 shows temperature dependent 3D-ARPES spectra obtained for EuO (100) at the Γ (a) and X (b) points. ARPES peaks at binding energies E_B of 1.0 – 3.0 eV and of 4.0 – 7.0 eV are attributed to the Eu 4*f* and O 2*p* states, respectively, based on a band structure calculation as well as the photoionization cross section [4, 5]. In the ferromagnetic phase below 71 K, every peaks shift to the lower binding energy side by about 0.2 eV than that in the paramagnetic phase. These energy shifts originate from the band splitting of the Eu 5*d* state due to the ferromagnetic transition. In addition, the top of the Eu 4*f* states at the Γ and X points is shifted away from the main 4*f* states and also the intensity increases. In contrast, the O 2*p* state is spitted into two bands below T_C. The bands at the higher and lower binding energies are attributed to the majority and minority spin states, respectively. Since the Eu 4*f* state is fully polarized, the 4*f* state mainly hybridizes with the majority spin state of O 2*p*. Therefore, the bonding and antibonding states of the Eu 4*f* and O 2*p* states are shifted to the higher and lower binding energy side, respectively. This result indicates that the origin of the ferromagnetic transition is strong hybridization between the Eu 4*f* and O 2*p* states.

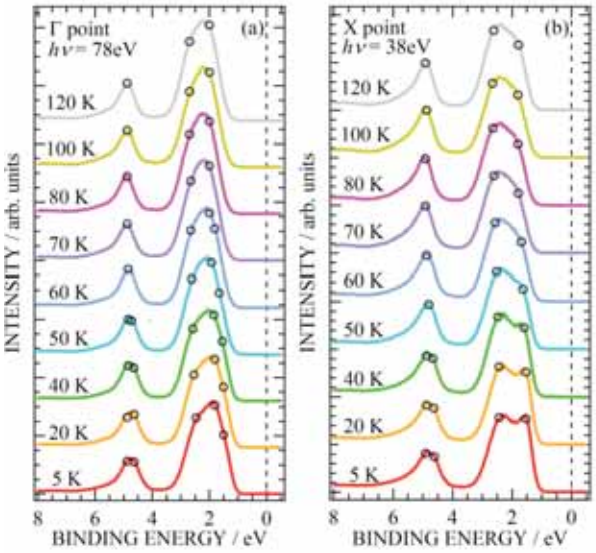

Fig. 1. Temperature dependence of the photoemission spectra of an EuO (100) thin film at the Γ (a) and X (b) points. The open circles indicate the peaks position evaluated from the second-derivative curveof each spectrum.

[1] N. Tsuda *et al.*, Electronic Conduction in Oxides (Springers College) (1976).
[2] A. Mauger *et al.*, J. Phys. (paris) **39** (1978) 1125.
[3] Y. Shapira, S. Foner, and T. B. Reed, Phys. Rev. B **8** (1973) 2299; Phys. Rev. B **8** (1973) 2316.
[4] H. Miyazaki *et al.*, Physica B **403** (2008) 917.
[5] J. J. Yeh and I. Lindau, At. Data Nucl. Data Tables **32** (1985) 1.

BL5U

Angle-Resolved Ultra-Violet Photoemission Study of $Fe_{2-x}V_{1+x}Al$

K. Soda[1,2], K. Nakamura[3], H. Miyazaki[1,2], M. Inukai[1], F. Ishikawa[4], Y. Yamada[4]
[1]*Graduate School of Engineering, Nagoya University, Nagoya 464-8603 Japan*
[2]*UVSOR Facility, Institute for Molecular Science, Okazaki 444-8585 Japan*
[3]*School of Engineering, Nagoya University, Nagoya 464-8603 Japan*
[4]*Faculty of Science, Niigata University, Niigata 950-2181, Japan*

Introduction

Heusler-type intermetallic compound Fe_2VAl shows unusual transport properties, which are reminiscent of the heavy fermion system [1]. The off-stoichiometric alloys $Fe_{2-x}V_{1+x}Al$ also reveal the remarkable enhancement in the thermoelectric power, which cannot be explained in terms of a rigid band model [2]. Theoretical studies suggest that the unusual properties may be induced by magnetic clusters around anti-site defects, whose *d* states appear within a sharp pseudogap across the Fermi energy E_F in its semimetallic electronic structure [3,4]. Thus, we have investigated the electronic structures of $Fe_{2-x}V_{1+x}Al$ using angle-resolved photoemission spectroscopy (ARUPS) in order to clarify the origins of the unique transport and thermoelectric properties.

Experimental

The ARUPS measurements were performed at BL-5U using linearly polarized synchrotron light as an excitation light source. Single crystalline specimens of $Fe_{2-x}V_{1+x}Al$ were prepared by the Czochralski pulling method in a tetra-arc furnace [2] and their clean (001) surfaces were obtained by *in situ* fracturing them at low temperatures.

Results and Discussion

Figure 1 shows ARUPS spectra of the $Fe_{2.05}V_{0.95}Al$ (001) surface recorded with the (010)-polarized 65 eV excitation light at various polar angles θ along the (100) axis, which elucidates the electronic structure along the Γ-X line. There are at least two prominent bands and three weak bands, whose peak positions are indicated by black solid circles in Fig.2, the image plot of the second derivative of the ARUPS spectra versus the wave vector. The band structure of Fe_2VAl calculated by a code Wien2k is also shown by white curves in the figure. In spite of the expected increase in the valence electron concentration for $Fe_{2.05}V_{0.95}Al$, no electron pockets are clearly observed at the X point. This might be caused by the small enrichment of Al in the growth of the single crystals and result in the observed positive thermoelectric power [2].

Detailed analysis near E_F around the Γ and X points will be reported elsewhere.

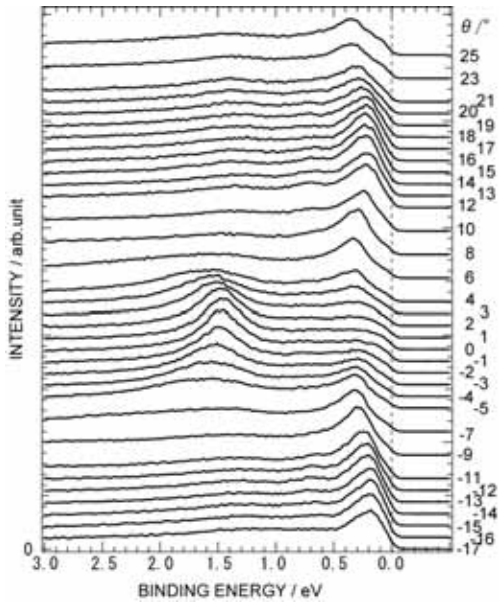

Fig. 1. Angle-resolved photoemission spectra of $Fe_{2.05}V_{0.95}Al$.

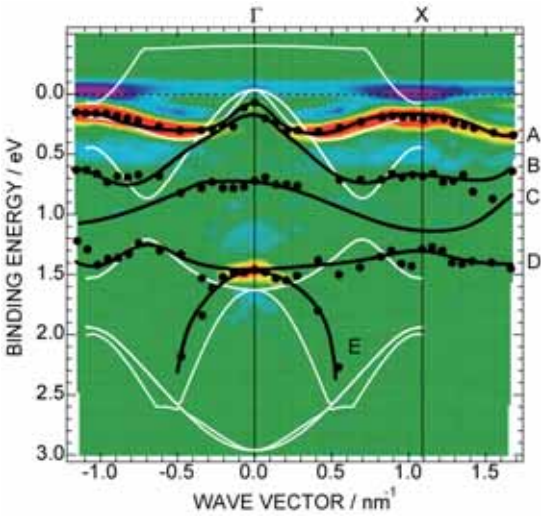

Fig. 2. Energy dispersion relation along the Γ-X line of $Fe_{2.05}V_{0.95}Al$.

[1] Y. Nishono *et al.*, Phys. Rev. Lett. **79** (1997) 1909.
[2] F. Ishikawa *et al.*, J. Magn. Magn. Mater. **310** (2007) e616.
[3] J. Deniszczyk, Acta Phys. Pol. B **32** (2001) 529.
[4] S. Fujii *et al.*, J. Phys. Soc. Jpn. **72** (2003) 698.

BL5U

Surface Chemistry of Alkyl-Passivated Si Nanoparticles Studied by Photoelectron Spectroscopy

A. Tanaka, N. Takashima, M. Imamura, T. Kitagawa, Y. Murase
Department of Mechanical Engineering, Graduate School of Engineering, Kobe University, Kobe 657-8501, Japan

Introduction

Numerous works focused on the optical properties of Si nanoparticles prepared by various methods have been reported to date. However, these optical properties in the literatures are ascribed to various sources, and this discrepancy is considered to originate that the physical properties of nanoparticles are greatly influenced by surface chemistry due to increase of surface area to volume ratio by reducing the size to the nanometer scale. In this paper, we have compared the valence-band photoemission spectra of fully *n*-butyl-passivated Si nanoparticles and those with oxygen contaminants in order to investigate their surface chemistry.

Experiment

Synthesis procedure of *n*-butyl-passivated Si nanoparticles used in this work is described elsewhere [1]. Photoemission measurements were performed at BL-5U of UVSOR II Facility for as-synthesized (fresh) *n*-butyl-passivated Si nanoparticles with mean diameter of d_c=1.1 nm and those exposed to ambient air for 10 minutes.

Results and Discussion

Figure 1 shows the valence-band photoemission spectra of as-prepared *n*-butyl-passivated Si nanoparticles with d_c=1.1 nm and those exposed to ambient air for 10 minutes, on the HOPG substrate at room temperature with photon energy of 195 eV. Spectral features in the photoemission spectrum of as-prepared *n*-butyl-passivated Si nanoparticles originate from the C *2sp*- and Si 3*sp*-derived valence electronic states. The valence-band maximum energy (HOMO) energy is estimated to about 2.2 eV below the Fermi level as shown by thin arrow on lower spectrum in Fig. 1. If the Fermi level is considered to be located in the middle of HOMO-LUMO gap, HOMO-LUMO gap of the present *n*-butyl-passivated Si nanoparticles with d_c=1.1 nm can be estimated to about 4.4 eV. This result agrees with the recent quantum Monte Carlo (QMC) calculation by Putzer *et al.* [2]. On the other hand, it is confirmed from the FT-IR spectrum that the exposure to ambient air of the present *n*-butyl-passivated Si nanoparticles induce the removal of surface-passivants of alkyl groups and subsequent passivation of oxygen. As shown in Fig. 1, the valence-band spectrum of Si nanoparticles with oxygen contaminants exhibits an additional feature centered around 2.6 eV in binding energy (as shown by thick arrow in Fig. 1). Putzer *et al.* have also reported the QMC HOMO-LUMO gaps of surface-passivated Si nanoparticles with and without oxygen contaminants, and have shown a significant decrease of HOMO-LUMO gap due to the oxygen contaminations [2]. Moreover, they have also calculated the density of states (DOS) in surface-passivated Si nanoparticles with various contaminants by means of local density approximation (LDA). When a double bonded contaminant such as oxygen and sulfur is added to Si nanoparticle, Si sp^3 network is considerably distorted and HOMO and LUMO change their nature significantly. As a result, HOMO and LUMO states localized in the vicinity of the Si=O double bond, and the modified DOS originated from the HOMO and LUMO appears near the Fermi level as the additional features. From the comparison with this theoretical LDA DOS, it is considered that the additional feature in the present photoemission spectrum of Si nanoparticles with oxygen contaminants is ascribed to the modified HOMO states by oxygen contaminations.

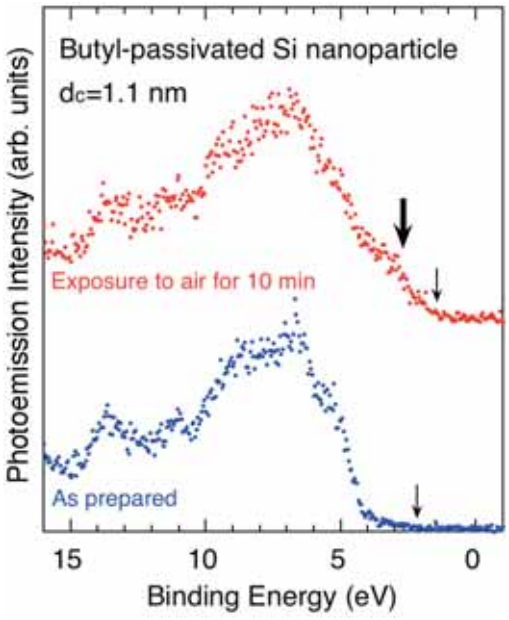

Fig. 1. Valence-band photoemission spectra of as-synthesized *n*-butyl-passivated Si nanoparticles with d_c=1.1 nm (blue) and those exposed to ambient air for 10 minutes (red).

[1] A. Tanaka *et al.*, Solid State Commun. **140** (2006) 400.
[2] A. Puzder *et al.*, Phys. Rev. Lett. **88** (2002) 097401.

BL7U

Momentum-Dependent Kondo Resonance Peaks in a Low-Energy Angle-Resolved Photoemission Spectroscopy

H.J. Im[1,2], T. Ito[2,3], H. Miyazaki[4,2], S. Kimura[2,3], C.I. Lee[1], K.E. Lee[1], Y.S. Kwon[1]

[1]*Department of Physics, Sungkyunkwan University, Suwon 440-746, Korea*

[2]*UVSOR Facility, Institute for Molecular Science, Okazaki 444-8585, Japan*

[3]*School of Physical Sciences, The Graduate University for Advanced Studies, Okazaki 444-8585, Japan*

[4]*Graduate School of Engineering, Nagoya University, Nagoya 464-8603, Japan*

For investigation of the electronic structure of strongly correlated electrons system, bulk-sensitive high-resolution angle-resolved photoemission spectroscopy (ARPES) with utilizing tunable photons has been a great challenge issue to physicists. In the case of cuprate superconductors, for instance, their electronic structures have been well surveyed with high energy resolution regardless of the bulk- or surface-states because of the two-dimensional electronic structure of CuO_2 layers which governs their physical properties [1]. On the other hand, the precise understanding of heavy-fermion systems requires the three-dimensional bulk electronic structure with high resolution [2]. This can be realized in a low energy photoemission using the synchrotron radiation source. Recently, the high resolution ARPES apparatus has been equipped in BL7U of UVSOR-II with photon energies from 6 to 40 eV [3].

Therefore, we have performed ARPES on $CeCoGe_{1.2}Si_{0.8}$, where the c-f hybridization bands were firstly observed in Ce 4d-4f resonant ARPES [4], as a target sample. The used photon energy is 15 eV, where the measured momentum spaces include Γ-point in normal emission. Total energy resolution is about 15 meV. Measurement temperature is 20 K which is very low compared to the Kondo temperature of $CeCoGe_{1.2}Si_{0.8}$ (T_K ~ 350 K). Sample surfaces were prepared by *in situ* cleaving under ultra high vacuum. Sample cleanliness is checked by the variation of spectral shape of valence which becomes broad due to surface contamination.

Figure 1 is the spectrum of valence band obtained in angle-integrated mode. We observed the two prominent spectral weights around -1.2 and -2.5 eV, and the tail of Kondo resonance peak at the Fermi-level. This indicates that Kondo resonance peaks composed of mainly f-state is well observed although the cross section of f-state is smaller than one of non-f-states (spd-state) in a low kinetic energy of photoelectrons.

Figure 2(a) is an intensity plot of ARPES spectra which represents a band dispersion. It is observed that a conduction band crosses the Fermi level at k = 0.2 $Å^{-1}$, where the evidence of c-f hybridization must appear as in Ce 4d-4f resonant ARPES [4]. Figure 2(b) shows the energy distribution curves at k = 0.07 and 0.2 $Å^{-1}$. The tail of Kondo resonance peak at the Fermi-vector (k = 0.2 $Å^{-1}$), while the corresponding feature is absent at k = 0.07 $Å^{-1}$. This indicates that Kondo resonance peak has the momentum dependence in agreement with a periodic Anderson model [4].

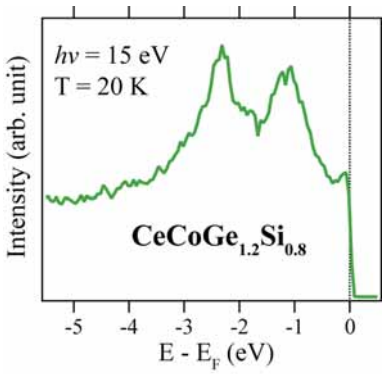

Fig. 1. Angle-integrated PES spectrum of $CeCoGe_{1.2}Si_{0.8}$ in valence band regime.

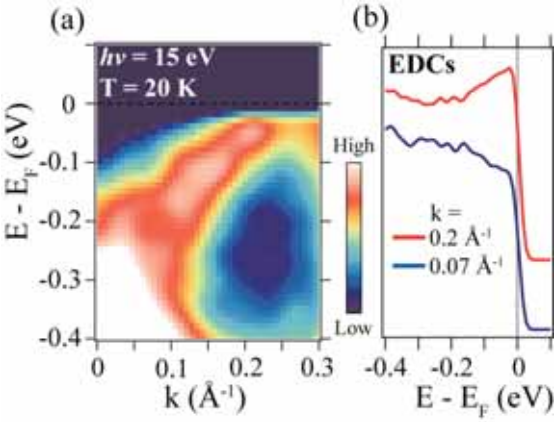

Fig. 2. (a) ARPES intensity plot of $CeCoGe_{1.2}Si_{0.8}$ at $h\nu$ = 15 eV. (b) Energy distribution curves at k = 0.2 and 0.07 $Å^{-1}$.

[1] A. Damascelli *et al.*, Rev. Mod. Phys. **75** (2003) 473.

[2] D. Malterre *et al.*, Adv. Phys. **45** (1996) 299.

[3] T. Ito *et al.*, AIP Conference Proceedings **879** (2007) 587.

[4] H.J. Im *et al.*, Phys. Rev. Lett. **100** (2008) 176402.

BL7U

Evidence of Three-Dimensional CDW Formation on $CeTe_2$: VUV Three-Dimensional Angle-Resolved Photoemission Study

T. Ito[1,2], H. J. Im[3], S. Kimura[1,2], Y. S. Kwon[3]

[1]*UVSOR Facility, Institute for Molecular Science, Okazaki 444-8585, Japan*

[2]*School of Physical Sciences, the Graduate University for Advanced Studies (SOKENDAI), Okazaki 444-8585, Japan*

[3]*Department of Physics, Sungkyunkwan University, Suwon 440-749, Korea*

Low-dimensional electronic structure is believed to be an important essence to understand the anomalous physical properties, such as a charge/spin density wave formation, high-*T*c superconductivity, etc., originating from the anisotropic electronic/magnetic structure. In turn, the investigation of the three-dimensional effect in the electronic structure is essentially important to understand the anomalous physical properties of low-dimensional compounds. To demonstrate the importance of three-dimensionality to insight into the anomalous physical properties, we have performed three-dimensional angle-resolved photoemission spectroscopy (3D-ARPES) on quasi-two-dimensional charge-density-wave (CDW) compound $CeTe_2$ [1] where the existence of three-dimensional anomaly at the Fermi surface (FS) has been reported [2].

The 3D-ARPES was performed at the beamline 7U of UVSOR-II, the Institute for Molecular Science, which has been developed in 2007 for bulk-sensitive ARPES on strongly correlated electron systems in the VUV region [3]. Taking account of the inner potential of $V \sim 16.4$ eV [2], we set the measurement axis along (110) plane of Te 5*p* hole-like FS (see hatched blue area in Fig. 1).

Figure 2 shows the evolutions of the hole-pocket around the MR line as a function of photon energy $h\nu$, in other word, of the k_z line in the Brillouin zone. We clearly observe that the Te 5*p* band (solid line) folds at the E_F crossing point (dashed line) at $h\nu = 19$ eV (ΓM line), *i.e.*, the Fermi surface of the Te 5*p* band is nested due to the CDW formation. Furthermore, with decreasing photon energy, the separation between the Te 5*p* band and the folded band gradually increases. This result suggests that the nesting condition becomes imperfect from the ΓM to ZR lines gradually. The observed change of the folded band certainly indicates the existence of the unexpected three-dimensional CDW vector in quasi-two-dimensional $CeTe_2$.

The origin of the observed three-dimensional CDW vector is not clear at present, since there are few examples of three-dimensional study of electronic structure so far, especially for the quasi-two dimensional materials. Present observation of three-dimensional interactions on quasi-two dimensional $CeTe_2$ clearly indicates that 3D-ARPES will shed light on understanding the effect of anisotropic interactions originating in the various functionalities.

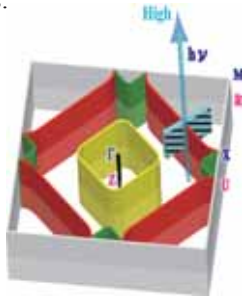

Fig. 1. Schematic Fermi surface of $CeTe_2$.

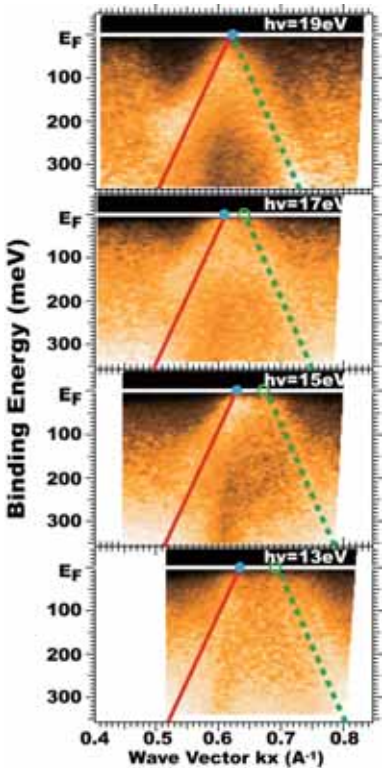

Fig. 2. $h\nu$-dependent experimental band structure of $CeTe_2$ The images of $h\nu = 19$ and 13 eV correspond to the band structure in the ΓM and ZR lines, respectively. See the text for details.

[1] M. H. Jung *et al.*, J.Phys.Soc.Jpn **69** (2000) 937.
[2] T. Ito *et al.*, J. Mag. Magn. Mater. **310** (2007) 431; Physica B **378-380** (2006) 767.
[3] S. Kimura *et al.*, AIP conf. Proc. **879** (2007) 527.

BL7U

Temperature-Dependent Extremely Low-Energy Photoemission Spectroscopy of a Fe-Based "Kondo Semiconductor"

A. Sekiyama[1], G. Funabashi[1], S. Komori[1], M. Kimura[1], M. Tsunekawa[1], H. Sugiyama[1], T. Uyama[1], H. Nakamura[2], T. Ito[3], S. Kimura[3], S. Imada[1], S. Suga[1]

[1]*Graduate School of Engineering Science, Osaka University, Toyonaka, Osaka 560-8531, Japan*

[2]*Graduate School of Engineering, Kyoto University, Kyoto 606-8501, Japan*

[3]*UVSOR Facility, Institute for Molecular Science, Okazaki 444-8585 Japan*

Introduction

Kondo semiconductor or Kondo insulator, which shows nonmagnetic semiconducting behavior at low temperatures with a formation of the (pesudo-)gap while it is rather metallic at high-temperature, is one of intriguing subjects in strongly correlated electron systems. $FeSb_2$ [1,2] is recognized as a candidate for the Kondo semiconductor, whose macroscopic properties are similar to those for already known 4f-based Kondo semiconductors. From previous photoemission studies [3], it has been known that the surface of the Kondo semiconductor is often metallic. Therefore, bulk-sensitive photoemission is very important to clarify their intrinsic electronic states. Recently, extremely low-energy photoemission (ELEPES, $h\nu < 10$ eV) has been thought as another possible technique [4] as bulk-sensitive photoemission, being complementary to high excitation-energy photoemission. We have performed ELEPES for $FeSb_2$ in order to examine the bulk electronic state.

Experimental

ELEPES was performed at BL7U by using a photoelectron spectrometer of MB Scientific A1 analyzer. In order to obtain clean surfaces, the bulk $FeSb_2$ samples were fractured *in situ*. We have measured both surface-sensitive and bulk-sensitive photoemission spectra by controlling excitation photon energies from 6.5 to 30 eV. The energy resolution was set to ~5 meV.

Results and Discussions

Figure 1 shows the temperature dependence of the ELEPES spectra measured at $h\nu = 6.5$ eV for $FeSb_2$. The spectra have been normalized by the spectral weight above the binding energy of 200 meV. At all measuring temperatures, the intensity monotonously decreased from the binding energy of 200 meV toward the Fermi level (E_F). In this energy region, the spectral weight is clearly reduced with lowering temperature. This indicates that the density of states near E_F decreases from 200 K in the metallic phase to 20 K in the semiconducting phase in the energy scale of 200 meV. Such temperature dependence is not seen in normal metals, suggesting that the electronic structure changes intrinsically with temperature. On the other hand, a clear Fermi cut-off is seen at 20 K. If it is assumed that the surface contribution in these ELEPES spectra is negligible, we can conclude that $FeSb_2$ is semimetallic at low temperatures, in other words, a Kondo semiconductor with the negative indirect gap.

There is a broad peak at the binding energy of about 200 meV in all photoemission spectra at $h\nu$ = 6.5, 10, 21 and 30 eV (not shown here) which we have measured at 20 K in the so-called semiconductong phase. When we normalized the spectra by the intensity of the broad peak, the Fermi cut-off intensity decreases rather discontinuously from $h\nu = 21$ eV to 10 eV whereas it is comparable between $h\nu = 30$ eV and 21 eV, and between $h\nu = 10$ eV and 6.5 eV, respectively. This discontinuous reduction of the cut-off might be ascribed to the higher bulk sensitivity of the photoemission at $h\nu \leq 10$ eV than that at $h\nu > 20$ eV.

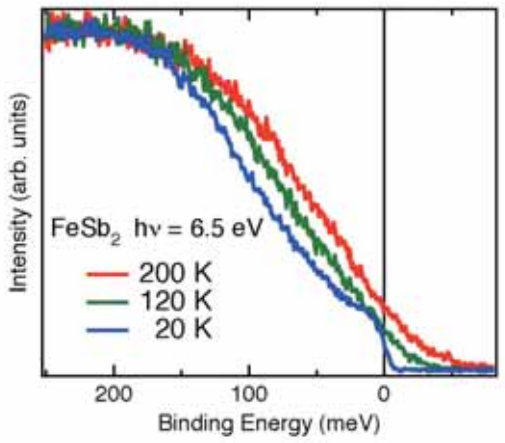

Fig. 1. Temperature-dependent extremely low-energy photoemission spectra of $FeSb_2$.

[1] C. Petrovic *et al.*, Phys. Rev. B **67** (2003) 155205.
[2] C. Petrovic *et al.*, Phys. Rev. B **72** (2005) 045103.
[3] For example, K. Breuer *et al.*, Phys. Rev. B **56** (1997) R7061.
[4] T. Kiss *et al.*, Phys. Rev. Lett. **94** (2005) 057001.

BL7U

Electronic Structure and Thermoelectric Power of $La_{2-x}Sr_xCuO_4$

T. Takeuchi[1,2], H. Komoto[2], T. Ito[3], S. Kimura[3]

[1]*EcoTopia Science Institute, Nagoya University, Nagoya 464-8603 Japan*

[2]*Department of Crystalline Materials Science, Nagoya University, Nagoya 464-8603 Japan*

[3]*UVSOR Facility, Institute for Molecular Science, Okazaki 444-8585 Japan*

Thermoelectric power of the cuprate superconductors is widely known to possess unusual behaviors such as the non-linear temperature dependence and the positive to negative sign-reversal with increasing hole-concentration. These behaviors are not generally observable for metallic compounds. Strong electron correlation is considered as one of the possible origins inducing such unusual behaviors in thermoelectric power.

By using the angle resolved photoemission spectroscopy (ARPES) and the semi-classical Bloch-Boltzmann theory, we revealed for the $Bi_2Sr_2CuO_{6+\delta}$ (Bi2201) and $Bi_2Sr_2CaCu_2O_{8+\delta}$ (Bi2212) superconductors that the unusual behaviors of the thermoelectric power, especially its large magnitude with positive sign in underdoped samples, are caused by the strong scattering of the conduction electrons at the anti-ferromagnetic zone boundary (AFZB). [1,2] Note here that the AFZB is essentially caused by the anti-ferromagnetic ordering of the conduction electrons, that is not fully observable in the superconductors but in the Mott-Insulator as a consequence of the carrier localization caused by the strong on-site coulomb interaction. Therefore, it is safely argued that the thermoelectric power of the cuprate superconductor is indeed characterized by the strong electron correlation.

One may wonder that the effects of the electron correlation on the thermoelectric power, that is caused strong scattering at the AFZB, could be closely related with the stability or instability of superconducting phase. To gain deeper insight into the relation between the strong scattering at the AFZB and superconducting transition temperature, we determined the development of the AFZB scattering of conduction electrons as a function of carrier concentration by analyzing thermoelectric power of the $La_{2-x}Sr_xCuO_4$ (LSCO) superconductors as we did for the Bi2201 and Bi2212 in our previous works. [1,2]

The single grained $La_{2-x}Sr_xCuO_4$ samples of $0.06 \leq x \leq 0.25$ were prepared by the floating-zone method. The superconducting transition temperature was determined by the magnetization measurement with the SQUID magnetometer. We also measured electrical resistivity and thermoelectric power with the Thermal Transport Option of the Physical Property Measurement System assembled by Quantum Design Inc. High resolution ARPES was performed at the BL05U of UVSOR, Okazaki Japan. The energy resolution employed in this study was ~20meV, which was defined by the energy with of intensity reduction from 90 % to 10 % at the Fermi level of reference gold electrically contacted with samples. The ARPES measurements were performed at 50K with the incident photon energy of 30.0 eV.

Figure 1 shows a typical example of the observed ARPES images together with the energy distribution curves and the momentum distribution curves which were cut from the image. The band dispersion is clearly observed, and we safely determined $\varepsilon(\mathbf{k})$ with employing the tight-binding function fitting of four different transfer integrals. Once $\varepsilon(\mathbf{k})$ is determined, spectral conductivity $\sigma(\varepsilon)$ can be calculated from $\varepsilon(\mathbf{k})$ under an assumption of constant mean free path as we assumed in our previous analysis on the Bi2201 and Bi2212. By taking the effect of the AFZB scattering into account, we calculated thermoelectric power of LSCO from the experimentally determined $\sigma(\varepsilon)$. Figure 2 shows calculated and measured thermoelectric power. The calculated thermoelectric power quantitatively reproduced the measured one even in their carrier concentration dependence. As a result of this calculation, we realized that the LSCO is more strongly affected by the AFZB scattering than the Bi2201 and Bi2212. This tendency must be caused by the smaller carrier concentration of LSCO than that of Bi2201 and Bi2212.

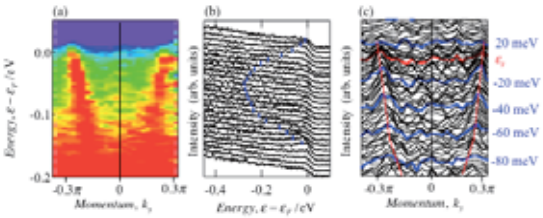

Fig. 1. (a) an ARPES intensity image near the (π, 0) point of $La_{1.75}Sr_{0.25}CuO_4$ accumulated at 50K. (b) Energy distribution curves and (c) momentum distribution curves cut from the ARPES image. A band crossing the Fermi level is clearly observed.

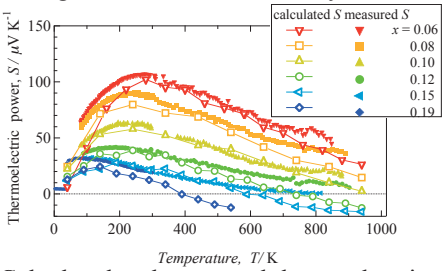

Fig. 2. Calculated and measured thermoelectric power of $La_{2-x}Sr_xCuO_4$. The measured value is quantitatively reproduced by the calculation.

[1] T. Kondo *et al.*, *Phys. Rev. B* **72** (2005) 024533.
[2] T. Takeuchi *et al.*, *J. Elec. Spec. Relat. Phenom.* **156-158** (2007) 452-456.

BL8B1

Graphitization of Thin Films Formed by Focused-Ion-Beam Chemical-Vapor-Deposition

K. Kanda, J. Igaki, N. Yamada, R. Kometani, S. Matsui
Laboratory of Advanced Science and Technology for Industry, University of Hyogo, Kamigori, Hyogo, 678-1205 Japan

Focused-ion-beam chemical-vapor deposition (FIB-CVD) method is developed as an effective technique for producing of three-dimensional nano-structures, which formed complex shape with overhung, hollow and bridging structure. In this method, scanning of focused Ga ion beam under the phenanthrene gas atmosphere using as a source gas leads to deposition of carbon material at arbitrary nano-scale area. The fundamental structure of carbon material formed by FIB–CVD is diamond-like carbon (DLC) from the measurement of Raman spectrum [1]. It was known that pillars grown by FIB–CVD had a Ga-rich core and these residual Ga departed from the FIB–CVD DLC by the annealing at 700°C. In the other hand, the pillar was reported to graphitize by the transfer of Ga using flash discharge [2].

The coordination of the carbon atoms has been principally determined by near-edge x-ray absorption fine structure spectroscopy (NEXAFS). The movement of Ga in the FIB-CVD DLC thin film by annealing was observed in the NEXAFS study [3], but the graphitization was not obviously confirmed. In the present study, FIB-CVD DLC films of ≈200 nm thickness were prepared by annealing at 1 hour in the temperature range from room temperature to 750°C. Fig. 1 shows the C K-edge NEXAFS spectra of FIB-CVD DLC films, (a) as deposition and (b) after 1 h annealing at 750°C with that of (c) graphite as a reference. The intensity of a peak at 285.4 eV, corrsponding to 1s→π* trangition increased by the annealing. This increase indicated that sp^2/sp^3 ratio increased in the film. In the 290-320 nm of σ* resonance region, the several bands characteristic to FIB-CVD DLC thin film changed by the annealing to the strctural bands characteristic to the graphite. These changes indicated that FIB-CVD DLC films graphitized by the 1 h annealing at 750°C.

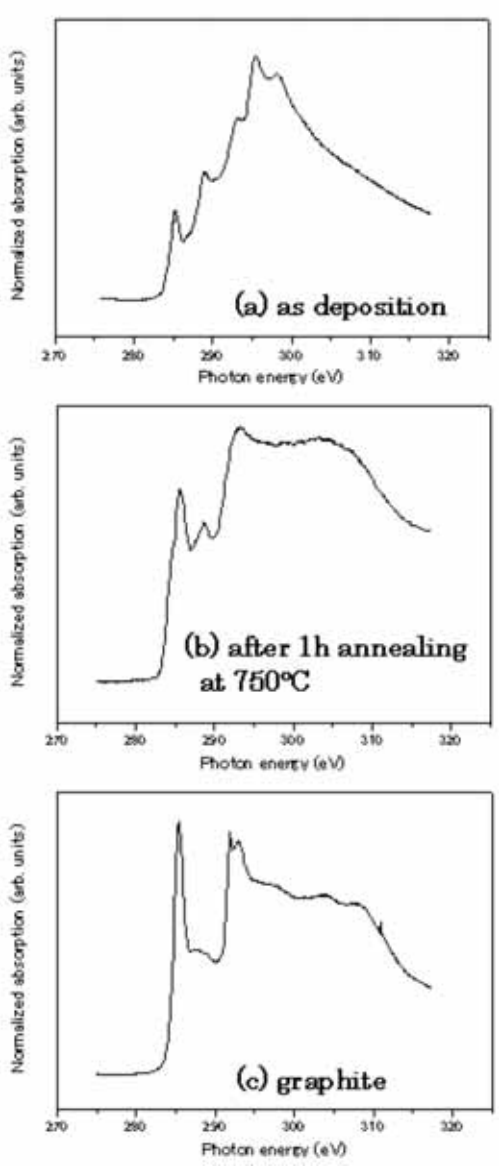

Fig. 1. C K-edge NEXAFS spectra of FIB-CVD DLC thin films and graphite.

[1] S. Matsui *et al.*, J. Vac. Sci. Tech. B **18** (2000) 3181.
[2] J. Fujita *et al.*, Appl. Phys. Lett. **88** (2006) 83109.
[3] A. Saikubo *et al.*, Jpn J. Appl. Phys. **46** (2007) 7512.

BL8B1

Characterization of Various Lithium Compounds by an XAFS Method

T. Kurisaki[1], Y. Sakogawa[1], D. Tanaka[1], H. Wakita[1,2]

[1]*Department of Chemistry, Faculty of Science, Fukuoka University, Nanakuma, Jonan-ku, Fukuoka 814-0180, Japan*

[2]*Advanced Materials Institute, Fukuoka University, Nanakuma, Jonan-ku, Fukuoka 814-0180, Japan*

Lithium compounds are used in industrial and commercial applications such as lithium ion batteries, lithium glasses, and medicines of a manic-depressive illness. The XAFS method has not been widely used to estimation the characteristic of these materials owing to the low energy (below about 70eV) of Li K edge. However, there are a few reports about Li-K XANES spectra [1].

In this work, we applied the X-ray absorption near edge structure (XANES) spectroscopy to lithium compounds. X-ray absorption spectra of near Li K absorption edges were (XAFS) measured at BL8B1 of the UV-SOR in the Institute of Molecular Science, Okazaki [4]. The energy of the UVSOR storage ring was 750MeV and the stored current was 110-230 mA. The absorption was monitored by the total electron yield using a photomultiplier. We employed the discrete variational (DV)-Xα molecular orbital (MO) method to obtain calculated spectra, and compared observed spectra with the calculated spectra.

The Li *K* XANES spectra for various lithium compounds are shown in Fig. 1. The energy was not calibrated by standard samples. The energy position of each first peak should not depend on the charge of anion. However, the peak shapes are different by the anions. This result showed that the two aluminum compounds have different electronic state. We are going to try to calculate the spectra by DV-Xα molecular orbital calculations

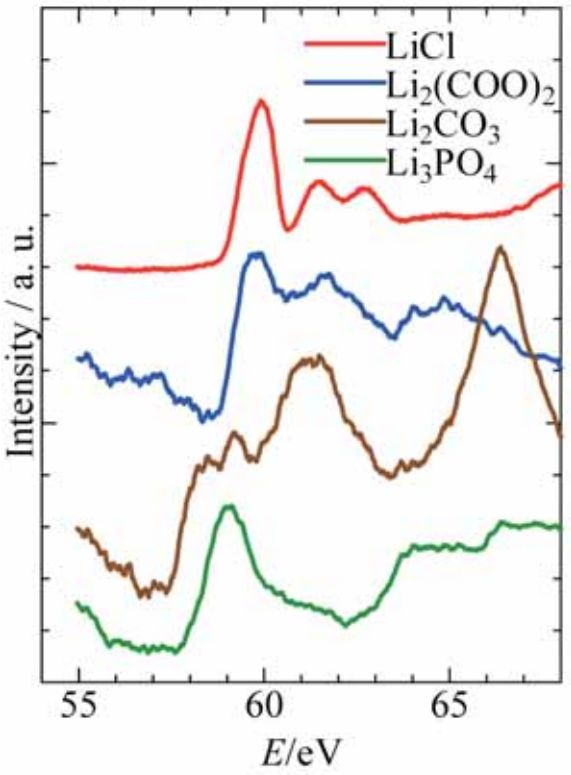

Fig. 1. Li K-edge XANES spectra of lithium compounds.

[1] J. Tsuji *et al.*, Adv. X-ray Chem. Anal. Jpn. **31** (2000) 149.
[2] J. Tsuji *et al.*, J. Synchrotron Radiat. **8** (2001) 554.
[3] J. Tsuji *et al.*, X-Ray Spectrom. **31** (2002) 319.
[4] S. Murata *et al.*, Rev. Sci. Instrum. **63** (1992) 1309.

BL8B1

N K-Edge XANES Analysis of Nitrogen Implanted in TiO_2

T. Yoshida[1], S. Muto[1], H. Yoshida[2]

[1]*Department of Materials, Physics and Energy Engineering, Nagoya University, Furo-cho, Chikusa-ku, Nagoya 464-8603*

[2]*EcoTopia Science Institute, Nagoya University, Furo-cho, Chikusa-ku, Nagoya 464-8603*

Photocatalytic reactions at the surface of titanium dioxide (TiO_2) under UV light irradiation have been attracting much attention due to their practical applications such as environmental cleaning. Recently, Asahi *et al.* reported that substitutional doping of nitrogen into TiO_2 contributed to narrowing of the band gap, thus providing a visible-light response [1]. Furthermore, previous investigations demonstrated that nitrogen doping generated new optical absorption bands in the visible-light region and the absorbance evolved with increasing nitrogen. On the other hand, absorbance may not be linearly proportional to the photocatalytic activity, and it is thus important to understand the chemical environment of N in TiO_2. In the present investigation, structural analysis was performed for N^+-implanted TiO_2 catalysts by means of X-ray absorption spectroscopy (XAFS).

The samples used in this study were TiO_2 (1 0 0) single crystals (5 x 5 x 0.5 mm^3), supplied by Furuuchi Kagaku, Japan. Mass analyzed 100 keV N_2^+ ions (50 keV/ N^+ ion) were injected into the samples at room temperature, perpendicular to the sample surface. The N^+ fluence ranged from 1 to 5 x 10^{21} m^{-2}. After the ion implantation, parts of the samples were heat-treated at 573 K for 2 hours in air.

A typical photocatalytic experiment consisted of placing the N^+-implanted sample in 0.5 ml of aqueous methylene-blue (MB) solution (9.8 μmol/L) and subsequent exposure to visible-light using a 15 W Xe lamp with a cut filter for $\lambda > 430$ nm. The light absorbance at $\lambda = 664$ nm after exposure for 2 hours was measured to estimate the photocatalytic activity of the samples.

N K-edge XANES spectra of the N^+-implanted TiO_2 samples were measured at the BL-8B1 station of UVSOR-II at the Institute for Molecular Science, Okazaki, Japan. Data were recorded at room temperature in total electron yield mode, and the X-ray energy dependence of the N Auger electron yield was monitored [2]. Considering the escape depth of the Auger electrons, the spectra probe the sample from the surface up to a few nanometers in depth.

The photocatalytic activity reached its maximum at a fluence of 3 x 10^{21} m^{-2} and then decreased with the fluence. The sample implanted at a fluence of 5 x 10^{21} m^{-2} followed by heat-treatment at 573 K was almost photocatalytically- inactive under visible-light irradiation.

Fig.1 shows the N K-edge XANES spectra of the N^+-implanted TiO_2 samples and a TiN powder. Similar XANES features for (a) and (b) suggest that N in the sample implanted by 3 x 10^{21} m^{-2} (highest active photocatalyst) is in a chemical environment similar to that in TiN. More thorough observation suggested that double-peak around 400 eV in (b) shifted to the lower energy side compared with that of TiN, which was well reproduced by the theoretical prediction using FEFF code [3] when N occupies one of the O sites of TiO_2, as suggested in ref.[1]. On the other hand, the XANES spectrum of the sample implanted with the N^+ fluence of 5 x 10^{21} m^{-2} followed by heat-treatment (almost inactive to visible-light) shows a distinct single peak at around 401 eV (Fig. 1c). This peak was attributed to formation of N̄O and/or N̄N bonds near the surface [3], which significantly suppresses the photocatalytic activity.

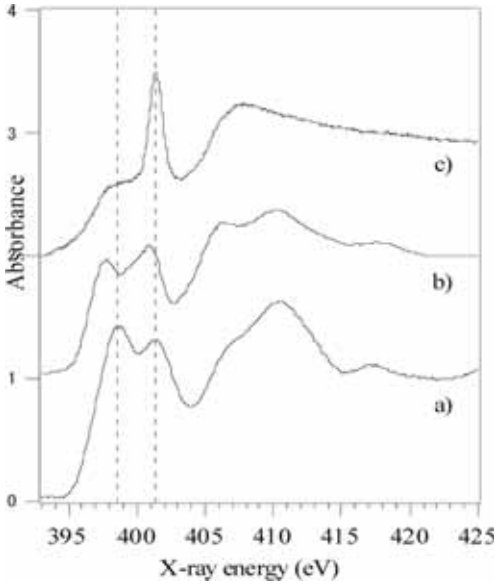

Fig. 1. N K-edge XANES spectra of a TiN(a), N^+-implanted at 3 x 10^{21} m^{-2}(b) and 5 x 10^{21} m^{-2} followed by heating at 573 K for 2 h(c).

[1] R. Asahi *et al.*, Science **293** (2001) 269.
[2] A. Erbil *et al.*, Phys. Rev. B **37** (1988) 2450.
[3] A. L. Ankudinov *et al.*, Phys. Rev. B **58** (1998) 7565; J. Stöhr, R. Jaeger, Phys. Rev. B **26** (1982) 4111.
[4] J.-H. Wang *et al.*, Anal. Chim. Acta **476** (2003) 93.